AMERICAN UNIVERSITY OF BEIRUT

EARLY DETECTION OF CORROSION IN REINFORCED CONCRETE STRUCTURES USING GUIDED WAVES TECHNIQUE

by
NURA USAMA HABBABA

A thesis
submitted in partial fulfillment of the requirements
for the degree of Master of Engineering
to the Department of Civil and Environmental Engineering
of the Maroun Semaan Faculty of Engineering and Architecture
at the American University of Beirut

Beirut, Lebanon
August 2023

AMERICAN UNIVERSITY OF BEIRUT

EARLY DETECTION OF CORROSION IN REINFORCED CONCRETE STRUCTURES USING GUIDED WAVES TECHNIQUE

by

NURA USAMA HABBABA

Approved by:

Dr. Samir Mustapha, Associate Professor Department of Mechanical Engineering	Advisor
Dr. Ye Lu, Associate Professor Department of Civil Engineering, Monash University	Co-Advisor
Dr. Darine Salam, Associate Professor Department of Civil and Environmental Engineering	Member of Committee
Dr. Mayssa Dabaghi, Assistant Professor Department of Civil and Environmental Engineering	Member of Committee

Date of thesis defense: August 16, 2023

AMERICAN UNIVERSITY OF BEIRUT

THESIS RELEASE FORM

Student Name: ____Habbaba____________Nura______________Usama_________

I authorize the American University of Beirut, to: (a) reproduce hard or electronic copies of my thesis; (b) include such copies in the archives and digital repositories of the University; and (c) make freely available such copies to third parties for research or educational purposes:

☐ As of the date of submission

☐ One year from the date of submission of my thesis.

☒ Two years from the date of submission of my thesis.

☐ Three years from the date of submission of my thesis.

_________nura habbaba_______________21/08/2023______________

Signature Date

ACKNOWLEDGEMENTS

First and foremost, I would like to thank my supervisor, Dr. Samir Mustapha, for his guidance, expertise, and invaluable support throughout the entire research process. His insightful feedback and encouragement have been instrumental in shaping this thesis.

I would also like to extend my appreciation to the members of my thesis committee, Dr. Darine Salam, Dr. Mayssa Dabaghi, and Dr. Ye Lu for their insightful comments and suggestions that have greatly improved the quality of this work.

I would like to express my deepest gratitude to my family, my husband, and friends for their encouragement and understanding throughout this journey. Their support has been a constant source of motivation and strength.

I am grateful for the financial support provided by the Middle East Partnership Initiative- Tomorrow's Leaders Graduate program at the American University of Beirut, awarded under grant number SNEAAC19CA0037. Their generous support has played a crucial role in the successful completion of this research project.

ABSTRACT
OF THE THESIS OF

Nura Usama Habbaba for Master of Engineering
Major: Civil and Environmental Engineering

Title: Early Detection of Corrosion in Reinforced Concrete Structures Using Guided Waves Technique

Reinforced Concrete is one of the most widely used composite materials in the modern construction industry for the building of infrastructure systems due to its availability of raw materials, low material cost, durability, fireproofing, and extended lifespan. Corrosion of reinforced concrete structures has become a significant problem worldwide, particularly in marine environments, resulting in exceptionally high maintenance costs. In the world of concrete failure, the actual cause is rarely visible, where only symptoms are visible due to accumulated internal stresses. These stresses may be generated due to corrosion of embedded reinforcement and may trigger partial or full collapse of the structure. Consequently, to maintain structural integrity and safety, robust non-destructive techniques to identify the initiation of corrosion are required.

Fiber Bragg Grating (FBG) sensors and ultrasonic guided waves (UGW) have emerged as significant technologies in the field of structural health monitoring as they are promising methods for corrosion monitoring in reinforced concrete. FBG sensors are optical sensors that may detect corrosion-induced stresses in concrete, whereas UGW monitoring has been proven to be sensitive to a wide range of faults in composite and metallic constructions. In addition, given that they can propagate for long distances, a larger area may be inspected with a handful of sensors.

In reinforced concrete buildings, corrosion causes delamination between the reinforcing steel and concrete interface, which in turn affects the wave propagation characteristics. This study presents an overview of recent developments in corrosion monitoring by using FBG sensors and UGW. The advantages and limitations of these approaches are examined, as well as their potential for real-time corrosion monitoring in reinforced concrete members. In this research, we aimed at detecting early corrosion in steel-reinforced concrete by relying on the leaking wave. Hence, UGW propagation in steel bars embedded in concrete and the inspection of leaked energy from one bar to another through propagating in the concrete medium was investigated experimentally and numerically. It also aims to provide passive corrosion monitoring using embedded FBG strain sensors. Since natural corrosion is a slow process, an accelerated corrosion setup is used to induce artificial corrosion in a reinforced concrete specimen using the impressed voltage approach. The results obtained showed that the amplitude of the first longitudinal mode L(0,1) propagating is extremely sensitive to the corrosion mechanism, even when monitored away from the source of corrosion as it varies with the progress of corrosion. It is shown that corrosion initiation can be detected successfully and different corrosion phases which are corrosion initiation, corrosion progression, and diameter reduction can

be detected from the signal strength and characteristics of L(0,1) as it is sensitive to corrosion defects along steel bars. Further, the leaking wave was sensitive to the diameter reduction phase and propagation of the cracks as the corrosion progressed. Additionally, the integration of FBG sensors provided further insights into the correlation between strain and GW readings, particularly during the diameter reduction phase.

TABLE OF CONTENTS

ILLUSTRATIONS

Figure

TABLES

Table

CHAPTER 1

OVERVIEW

1.1 Concrete Structures and Their Failure Modes

The period during which concrete was invented is contingent upon the interpretation of the term "concrete." In ancient times, structures were built using crushed gypsum or limestone, while mortar was a combination of these materials with sand and water, creating a plastering substance used for binding stones during construction. Over time, these materials were refined and mixed with other components, evolving into modern concrete. The history of concrete spans over 5,000 years, from the construction of the Egyptian Pyramids to modern artistic concrete. Concrete has played a significant role in various impressive constructions throughout history. The Egyptians used early forms of concrete, made from gypsum, lime, and bricks of straw and mud, to build the Pyramids over 5,000 years ago. The ancient Romans also used a substance similar to modern concrete in their architectural marvels like the Colosseum and Pantheon. They even used animal products as additives to achieve specific material quality, which is still used in modern concrete [1]. Today, plain cement concrete (PCC) is the common form of concrete, consisting of cement, water, fine and coarse aggregates, and admixtures.

This commonly used material is inherently weak in tension, making it a brittle material that is not able to resist tensile forces caused by wind, earthquakes, and vibrations. To address this limitation, steel reinforcement is embedded within the concrete structure in the form of bars, mesh, cables, or wires. This combination of concrete and steel creates reinforced concrete (RC), thus this combination will improve the overall strength of concrete against many types of loading by combining the compressive strength of concrete and the tensile strength of steel [2]. The bond between steel and concrete allows them to function as a unified structural unit, capable of resisting various applied forces [3]. The concept of RC emerged in the late 1800s, attributed to Joseph Louis Lambot, a French gardener who combined cement mortar with iron rods to construct water tanks, which he called ferro-cement [4]. Initially, advancements in RC were based on empirical observations, but in the 20th century, scientific understanding and analysis of this construction material developed further [5].

Reinforced Concrete (RC) is a widely used composite material in modern construction due to its availability, cost-effectiveness, durability, fire resistance, and long service life. Properly mixed, installed, and maintained RC structures can last up to 100 years. However, any structure, including RC, is susceptible to partial or complete loss of integrity and load-bearing capacity, leading to failure or collapse. The supportive steel reinforcement may be either passive, as normal reinforcement, or active which is known as prestressed concrete, where reinforcement bars are stressed before external loading [6]. Buildings, towers, highways roads, bridges, tunnels, dams, precast structures, floating structures, and all conceivable structures are constructed using RC due to its robustness, availability, relatively low cost, ease of casting, and fire resistance.

In the world of concrete failure, the actual cause is rarely visible, where only symptoms are visible due to accumulated internal stresses. Internal stresses gradually accumulate within the structure, leading to various types of failure that can result in partial or complete collapse. Previous research indicated that the main problems experienced with concrete include:

1.1.1 Cracking

Cracking in concrete structures is a prevalent issue encountered by a larger number of engineers compared to other problems. These cracks can occur due to factors such as excessive loads, shrinkage, thermal expansion/contraction, or inadequate reinforcement. The widespread occurrence of cracks highlights the importance of addressing this particular concern in the design, construction, and maintenance of concrete structures [7].

1.1.2 Structural Collapse

This occurs when the concrete structure is unable to withstand the imposed loads, leading to a partial or complete failure. The connection between structural members plays a critical role in transferring loads from the top of the structure to its bottom supports where any errors in design, detailing, or inadequate supervision during the casting process can result in improper connections between structural components, which ultimately leads to insufficient load transfer. Consequently, this can result in either partial or complete collapse of the structure [8].

1.1.3 Spalling

Concrete spalling refers to the chipping, flaking, or peeling of the concrete surface, often exposing the underlying reinforcement. It is a common issue that occurs due to various factors and can affect both new and existing concrete structures [9]. Spalling typically starts with the formation of small cracks on the surface, followed by the detachment of concrete layers. Several factors contribute to concrete spalling like poor construction practices, freeze-thaw cycles, fire exposure, and chemical exposure.

1.1.4 Soil Failure

All structures are supported on a foundation that transfers the loads from the superstructure to the underlying ground. The type of foundation depends on the specific soil conditions at the construction site and can range from shallow foundations to deep foundations, raft systems, or piles. The bearing capacity of the soil, which determines its ability to support the structure, is influenced by factors like soil type, density, and shear strength. When the shear stresses within the soil exceed its shear strength, the soil will experience failure, potentially resulting in the tilting or collapse of the structure [10].

Moreover, the collapse of RC structures during the construction phase is a concerning problem, considering that the construction period is relatively short compared to the lifespan of the building. Unfortunately, there have been numerous incidents of collapse reported. These repetitive failures demonstrate the significance of this phase and emphasize the importance of ensuring proper construction practice [11]. Additionally, chemical reactions coming from weathering or environmental conditions may weaken the concrete matrix thus leading to failures under severe and continuous exposure. Similarly, excessive heat generated from fires can impact concrete characteristics where extremely high temperatures will lead to serious expansions and deteriorations in concrete.

Nowadays, the improvement and functionality of society are highly related to the use of superstructures such as buildings, dams, tunnels, and bridges that are frequently subjected to both static and dynamic loads, as well as environmental factors, resulting in additional significant stresses. Furthermore, it remains important to investigate why modern RC structures tend to have a relatively shorter service life compared to ancient structures like the Pantheon in Rome and the Pyramid of Giza, which have exhibited exceptional durability. Noting that the key distinction lies in the use of steel reinforcement embedded in concrete [12].

The reinforcing steel is used to compensate for the weak tensile resistance of plain cement concrete, its similar thermal behavior to concrete, its availability, and its low cost. However, steel has a serious weakness; its susceptibility to rusting. The corrosion not only reduces the strength of the reinforcement, but its by-product, iron oxide, expands where this expansion causes stresses in the surrounding concrete, which eventually leads to cracking, delamination, spalling, and may reach a complete loss of serviceability (Figure 1)[12].

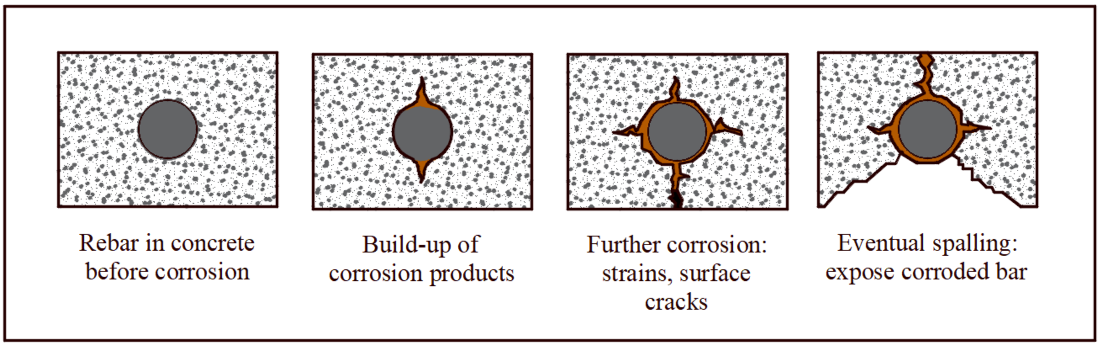

Figure 1 Corrosion-induced stresses

Hence, the deterioration of concrete due to corrosion of embedded steel, which dramatically reduces the service life, durability, performance, and safety of structures if not detected early and properly maintained, has emerged as one of the challenges facing the construction industry. The maintenance and repair of deteriorated concrete structures consume energy and resources resulting in a multi-billion-dollar infrastructure deficit [13]. The cost of repairing corroding concrete bridges in the United States, for example, was estimated to be $24 billion in 1986, with an increase of $500 million annually [14].

One of the major contributors to the corrosion of steel reinforcement is chloride attack, where chloride ions will be present because of the use of chloride-contaminated components or equipment, the use of $CaCl_2$ as an accelerator in concrete mix design for high early strength development, or diffusion into the concrete from the surrounding environment, particularly in coastal regions with high chloride concentrations. Chloride attack is special because it acts primarily on corroding the steel reinforcement, and the surrounding concrete is only damaged because of the corrosion process [15].

The damage due to the corrosion of steel reinforcement embedded in concrete is typically observed as spalling and cracking of the surrounding concrete as a result of internal stresses generated by the increased volume of the corroded reinforcement [16]. Under normal conditions in uncontaminated concrete, a passive film is formed on the rebar surface, acting as a barrier against corrosion, due to the alkalinity (PH value is 12.6~13.6) of cement paste during concrete casting where the steel remains unchanged and protected as long as the passive film is present. However, the penetration of chloride ions to the steel surface will lead to the de-passivation of the protective layer and the occurrence of oxidation reactions due to reduced PH values, allowing corrosion to start [17, 18]. The corrosion process of steel in the presence of oxygen and water can be summarized by the following chemical reactions:

Anodic Reaction: $Fe_{(s)} \rightarrow Fe^{2+} + 2e^-$

Cathodic Reaction: $2H_2O + O_2 + 4e^- \rightarrow 4OH^-$

Overall Reaction: $Fe^{2+} + 2OH^- \rightarrow Fe(OH)_2$

$4Fe(OH)_2 + O_2 + 2H_2O \rightarrow 4Fe(OH)_3$

The rust formation results in an increase in the volume where the corrosion product resulted may occupy up to 6-10 times the volume of the original steel bar [19], thus crack formation due to generated internal stresses [17, 20]. When corrosion occurs, it starts with primarily maintenance and cost problems, but as time passes, it evolves into a safety issue that is more difficult to handle. As a result, efforts are needed to achieve the greatest feasible chloride penetration control. However, occasionally, this penetration is uncontrolled, and it will be discovered later when symptoms start to appear on the structure since corrosion may start without visible indication till it reaches concrete. So, to avoid being late in corrosion detection, the initiation of corrosion should be recognized as early as possible to select appropriate protective measures to control subsequent deterioration [14]. Hence, structural health monitoring (SHM) has been intensively investigated in recent years because of its feasibility and importance in early non-destructive monitoring and damage detection, where the literature reported a variety of techniques that were suitably employed for monitoring and assessment of concrete health destructively or nondestructively [17].

1.2 Inspection of Concrete Structure Using Various NDT Techniques

Researchers and engineers are working on assessing existing concrete structures to address the significant issue of structural integrity, with a focus on evaluating the compressive strength to ensure its safety and provide a clear image of the health of the concrete, as any deterioration will eventually affect its compressive strength. Numerous destructive and non-destructive techniques can be used to estimate the mechanical properties of concrete. The main objective is to investigate the service life and to detect any weakness in the structure strength. The standard destructive test involves the crushing of concrete cylinders to estimate mechanical properties and investigate service life, including crushing concrete cylinders and conducting tensile, bending, and compressive tests on laboratory samples [21]. Although this kind of testing is simple to conduct, simple to interpret, and produces useful information, it requires crushing the concrete, which makes it a non-repetitive test. So, it is not always the best method to use when evaluating concrete structures owing to the fact that in some cases, it affects the durability and lifespan of the structure.

Engineers have shown a growing interest in non-destructive methods for evaluating the health of concrete. The main objective of non-destructive testing (NDT) is to assess in situ properties like density, durability, crack depth, and moisture content without impacting the structure's serviceability. It is important to differentiate between non-destructiveness and non-invasiveness in these tests. While some non-destructive techniques may involve invasive procedures, they are considered non-destructive as long as they do not compromise the future usefulness of the component [22]. Structural and civil engineers employ various non-destructive techniques to monitor and evaluate changes in concrete structures where some of these methods are listed below:

1.2.1 Optical Methods

Visual inspection is a well-known optical inspection approach for assessment as the appearance of deteriorated areas can provide valuable information about the cause and severity of the damage. However, this method relies heavily on the operator's expertise and is limited in detecting surface damages, while damages can occur at any location that cannot be visually inspected [23]. Non-destructive optical methods that are appropriate for determining the strength of any concrete structure involve a variety of measuring techniques and tools like microscopes, endoscopes, video scopes, specialized geodetic equipment, tv cameras, etc. One can acquire a 3D image of the concrete surface using such techniques and analyze these detailed images using computer programs [24]. While optical methods are useful for evaluating a material's geometry, structure, and some mechanical parameters, they are not effective in determining the material's chemical composition or accurately quantifying failures.

1.2.2 Penetration resistance method

Using previously established correlations, penetration resistance methods are invasive NDT procedures that investigate the strength characteristics of concrete. In these techniques, probes are tried to push into concrete samples with a consistent force. By using correlations, determining the probe's penetration depth can reveal information about the compressive strength of concrete. Despite disturbing the concrete during penetration, the tests are regarded as non-destructive due to the minimal impact of the penetration on the structural integrity of the probed sample. It should be noted that the Windsor probe system is the most widely used penetration resistance technique [25].

1.2.3 Acoustic Methods

The impulse response method. In this method, the tested structure is struck with the calibrated rubber-tipped hammer at various measuring points that are usually spaced every 1000 mm, creating an elastic wave in the tested element. Then the geophone records and the amplifier simultaneously amplify the elastic wave signal that is propagating through the element. Following the processing of the recorded signals, the final test results are displayed as maps that show the distribution of the values of the characteristic parameters under investigation [26]. The method is useful for detecting voids in RC and deformations at the interface between layers, as well as locating defective areas and concrete inhomogeneity and this test is effective in massive concrete members reaching up to 1500 mm thickness [27].

Impact-echo method. An electromechanical transducer is used in the impact-echo system to produce a short pulse of ultrasonic waves that spread into concrete plate structures. Materials with different characteristics like concrete cracks, concrete air, concrete rebar, or external boundaries will reflect the stress pulse which will be received by the transducer which also serves as a receiver. Finally, the received signal will be shown on the oscilloscope and the received signals will be analyzed in the time domain or frequency domain [25]. The impact-echo system is a recent advancement in ultrasonic techniques that helps to measure the concrete thickness and is used to locate cracks, voids, and delamination.

Ultrasonic pulse velocity method. Ultrasonic pulse velocity methods measure the amount of time it takes for waves to travel between a sending and receiving point while propagating ultrasonic waves through solids. Using previously established correlations, and mathematical relationships, the characteristics of ultrasonic wave propagation can be used to characterize a material's composition, structure, elastic properties, density, and geometry. Also, by observing the scattering of ultrasonic waves, this non-invasive method is used to identify and characterize material flaws in addition to the severity of their damage [28]. The transmitting transducer is placed on the concrete surface and allows an ultrasonic pulse to travel through the concrete specimen and is detected by a receiving transducer at the opposite side. The velocity of the wave pulse can be calculated using the distance between the two points and the time taken for wave propagation, thus providing a detailed account description of the member strength under exploration.

1.2.4 Radiological methods

The intensity of an X-ray or gamma-ray beam attenuates as it penetrates through any material due to the scattering and absorption of the rays by the material. Consequently, the amount of radiation absorbed is determined by the radiation's quality, the material's density, and the member thickness. RC is a non-homogeneous low-density material, and it is reinforced with high-density steel reinforcement. As a result, radiography can be used to locate the reinforcement and determine its diameter and depth from the surface. Also, it can show the existence of voids, cracks, and foreign objects. Additionally, the maximum thickness that can be feasibly radiographed is 500 mm which makes it the main limitation of using radiography in concrete assessment due to high the dimensions of RC members in real structures [29]. Also, the interpretation of radiographs is a bit challenging since there is no common terminology to analyze the results.

1.2.5 Infrared Thermography

Infrared Thermography (IRT), commonly known as thermal imaging is a method of detecting thermal radiation emitted by materials where it generates an image of surface temperatures from the emitted radiation by an object or structure where the intensity of emitted radiations depends on the structure material and properties. It is a non-destructive testing technique that is accurate and efficient in the detection of voids, delamination, and other flaws in concrete structures. It is based on the idea that heat moves more slowly through voids and cracks than it does through solid RC. These variations in heat movement result in localized variations in surface dissipating temperature [30].

1.2.6 Terrestrial Laser Scanning

Laser scanning can accurately collect three-dimensional (3D) topographic data of a structure. The basic principle of laser scanning is based on the emission of a laser beam to measure the distance between the emitter and the surface of an object based on the time it takes for a signal to travel from transmission to reception. The output is a point cloud, which is a dataset of (x,y,z) coordinates that will be gathered, resulting in a 3D image of the structure [31]. It is a non-destructive approach that is commonly used to quantify displacements of entire structures or specific components over time where these displacements may be within acceptable or non-acceptable ranges that will arise an alert in the latter case.

These are some of the non-destructive testing techniques that are used to generally evaluate concrete structures, whether they are new or old. The primary uses of NDT for new buildings under construction are expected to be for quality control purposes regarding the quality of materials or construction works. On the other hand, the assessment of existing structures is often associated with the examination of structural integrity or serviceability. In any scenario, destructive testing alone may only allow a limited number of tests to be performed, which may be deceptive. As a result, the scientific community is working hard to develop trustworthy analytical procedures for non-destructive monitoring technologies.

CHAPTER 2

LITERATURE REVIEW

2.1 Literature Review

Reinforced concrete has been used as a cost-effective building material in civil engineering constructions. However, the environment has a significant impact on concrete. One of the serious effects is the corrosion of embedded steel reinforcement, which is currently a major issue globally, particularly for construction workers exposed to harsh environments. Over the past three decades, the severity of this problem has increased significantly [32]. Over the past 25 years, many practices in reinforced concrete design have been developed to counteract corrosion and its consequences. To maintain serviceability and safety standards for the intended use of any structure, the corrosion process must still be carefully monitored over time. Also, the construction industry is aiming to extend the service life of RC structures to over 100 years, which enhances the demand for corrosion monitoring as it is one of the main reasons behind concrete deterioration [33]. Consequently, there is a need for effective and nondestructive structural health monitoring systems for corrosion.

Review of previous failure data, visual inspection, electrochemical methods, ultrasonic testing, radiography, ground penetrating radar systems, and Infrared thermography are some of the techniques reported in the literature that may be useful for corrosion monitoring of steel reinforcement embedded in concrete [23]. A well-known inspection approach for assessing corrosion damage on the surface of concrete structures is visual inspection. The appearance of the corroded region can reveal important information about the source and severity of corrosion. It is the most popular approach; however, it is completely dependent on the operator's knowledge, and it is limited in detecting surface stains where corrosion can occur at any location that cannot be inspected visually until the concrete strength is severely compromised [34]. The most often used reinforcement corrosion monitoring techniques are electrochemical measures, which take full advantage of the electrochemical characteristic of the steel corrosion process, for example, measuring corrosion potential E_{corr} and resistivity maps where these potential maps reveal the zones that are most likely to undergo corrosion. However, they can only describe the possibility of corrosion occurrence and cannot describe the exact rate or the total quantity of corrosion [35]. Radiography monitoring is based on the passage of radiation, such as X-rays or gamma rays through a structure, and the resulting degrees of attenuation in these rays will vary depending on the structure's condition. Radiography procedures are quite accurate; nevertheless, all sides of the structure under monitoring must be accessible to perform radiographic measurements, which cannot be always accessible. Also, additional safety measures for the operator may be necessary depending on the type of radiation being utilized, where the side effects of excessive exposure of workers are still unknown [36]. Another NDT method of corrosion monitoring is ground penetrating radar systems (GPR) used in the condition assessment of RC due to its low-cost, high-efficiency, and non-destructive way. The emitted electromagnetic wave propagates through the structure until it reaches an interface between two materials, where the wave will be reflected and the strength of the reflected wave depends on the properties of the material [37]. A sub-surface inspection method infrared thermography (IRT) is used for corrosion detection in concrete reinforcement. One of the good indicators for the structural health of the RC structures is temperature where deformations, cracks, or corrosion will cause abnormal temperature distributions. With the development of new generations of infrared cameras, Infrared Thermography seems to be a more accurate, dependable, and cost-effective approach for reinforcement corrosion monitoring. However, like the GPR approach, the results are only qualitative where a greater level of corrosion leads to stronger IR thermal distributions [38]. Also, the acoustic emission (AE) technique is a passive technique used for monitoring concrete expansion and cracking features that result from excessive corrosion of steel reinforcement. As corrosion products accumulate around steel reinforcement in concrete constructions, stresses will be generated on the surrounding concrete. Cracks will develop when these stresses are strong enough to break the interface bonding, resulting in stress waves that are directly detected by AE sensors installed on the concrete surface [37]. On the other hand, due to the low corrosion energy release, acoustic emission is not sensitive to the initiation and early stages of corrosion [32]. So, some methods are costly or require a significant commitment of time or labor, whereas others may not provide complete and accurate information about the corrosion state of the object being monitored [23].

More effective and advanced monitoring techniques are being developed for the corrosion, strain, and cracking monitoring of steel in RC structures. A variety of optical fibers have been intensively studied for steel reinforcement monitoring including FBG sensors which are new types of sensors being developed in the 21st century [37, 39]. Small size, light weight, flexibility, high durability, immunity to electromagnetic interference, and ease of installation make FBG attractive for SHM as a non-destructive technique (NDT).

The suitability of FBG sensors to measure strain in RC structures due to corrosion has been thoroughly investigated. FBG sensors were used for strain monitoring due to corrosion of a steel bar and the effect of Polydimethylsiloxane (PDMS) coating on the sensing effectiveness was examined [17]. It was proved that coated FBGs with PDMS are more sensitive to corrosion detection than non-coated ones. FBG was employed as a strain sensor to monitor rust formation in concrete specimens during the corrosion process as rust formation will increase the volume in localized areas [40]. The research was conducted to correlate rebar weight loss, which represents corrosion rate, to the peak wavelength shift of the FBG sensor, noting that one FBG sensor was used to monitor the corrosion of twin steel rebar elements, where it was shown that the wavelength shift was increasing as the corrosion progresses [41]. FBG sensors were attached to steel rebar and covered with polystyrene foam to detect the FBG wavelength shift versus the percentage of reinforcement corrosion where the polystyrene foam act as good protection for the fiber during concrete pouring and hardening processes [3]. FBG was used sensor to monitor the strain of prestressed steel strands due to corrosion which affects the fatigue life, which decreases significantly as the corrosion rate of steel strands increases [42].

Although FBG sensors have been widely investigated for their suitability to measure strain in RC structures due to corrosion, one major limitation of FBGs is that they only allow the monitoring of stresses in particular locations of the concrete member under which the FBG is placed. Recently, wave-based techniques for monitoring RC structures by measuring changes in wave properties caused by corrosion have been deeply investigated. These techniques can be classified as active or passive monitoring techniques based on their mode of application and monitoring. Active monitoring includes the external stimulation of a wave into the structure to be monitored where the propagation of the wave is studied and the variations in the wave properties are investigated [43]. Hence, these variations can be related to damage and delamination. Passive monitoring approaches such as the acoustic emission technique mentioned before require the placement of sensors on the structure without any external stimulation and monitoring of the changes in the structure as damage progresses [14].

Ultrasonic waves have emerged as a significant active method for monitoring and assessing RC structures. The ultrasonic pulse velocity method has been employed to study the compressive strength of structural lightweight concrete, considering the variability of various factors [44]. UGW monitoring is one of the most important active ways for monitoring reinforced concrete evaluation and assessment. This approach involves the excitation of a high-frequency wavelet packet into a structure and then observing the transmission and reflection of the waves. The steel bar embedded in concrete serves as a waveguide, aiding in the transmission of wave packets where the transmitted wave properties will vary when the bar deteriorates due to corrosion [43]. The delamination or debonding was studied using both low-frequency (100 kHz) and high-frequency (1 MHz) signals, where the low-frequency fundamental mode was chosen for excitation because it was the least attenuative of L(0,1) at 100 kHz which is a surface sensitive mode capable of detecting corrosion's debonding action. However, the L(0,7) mode at 1 MHz is core sensitive at high frequency with low attenuation and minimal leakage into the surrounding concrete [15]. So, these modes were chosen for monitoring rebar corroding in an RC beam specimen. For external wave excitation, transducers coupled to both ends of a 25 mm bar diameter embedded in concrete were utilized, and it was stated that UGW can monitor debonding of concrete due to accumulated corrosion of steel rebar. Additionally, different longitudinal modes at low (<200 kHz) and high (2-8 MHz) frequencies were employed to monitor damage in RC specimens subjected to corrosion, and it was shown that the low-frequency mode was more sensitive to bond degradation between steel and concrete. The L(0,1) mode was discovered to be undetected in the early phases of corrosion when the F(1,1) mode was identified [33]. Whenever corrosion builds between the steel and the concrete, cracking begins and gradually progresses to the cover. As a result, debonding will begin to occur on specific areas of the bar, and signals will get stronger, making the L(0,1) mode more detectable. It was concluded that low frequencies were more sensitive to damage since they are transmitted along the surface of the bar where the corrosion usually starts. Furthermore, high-frequency (5 MHz) guided longitudinal waves were employed to monitor RC specimens undergoing both accelerated uniform and localized corrosion [45]. High-frequency longitudinal waves were selected due to their high propagation velocity, allowing them to travel long distances. The energy of these waves is concentrated mainly in the core of the rebar, resulting in minimal leakage into the surrounding mortar which makes it sensitive to rebar cross-sectional area loss during uniform corrosion. Moreover, the UGW technique was adopted to monitor the damage evolution due to corrosion of 20 mm steel rebar embedded in concrete. Based on the dispersion curves of a 20 mm bar diameter embedded in concrete, the L(0,1) mode was selected at an excitation frequency of 40 kHz where in this study, the amplitude of the first wave packet was only observed where it showed a gradual decrease as the corrosion process proceeded [32]. Another study investigated the effect of debonding levels between steel bars and concrete on the transmitted wave using a 120 kHz excitation frequency and a five-cycle sinusoidal wave [46]. Before pouring concrete, PVC pipes were wrapped around steel to simulate delamination. At this frequency, the longitudinal, flexural, and torsional modes L(0,1), F(1,1), and T(0,1), exist, respectively. However, L(0,1) is the first wave in the received signal since it has the highest velocity, so the first peak was studied for different delamination lengths. Furthermore, it was determined that lower frequencies were more susceptible to damage than higher frequencies. A 120 kHz excitation frequency was used to evaluate the change in the wave amplitude caused by various lengths of artificial defects in an 18 mm diameter steel rebar embedded in concrete to represent corrosion [47]. Only L(0,1), T(0,1), and F(1,1) may be generated at 120 kHz where theoretically, L(0,1) with the highest velocity will be the first wave signal received and from this perspective, the amplitude of the first wave packet was monitored for different defects. Another study proposed using the UGW to detect pitting corrosion in a 20 mm diameter rebar in concrete [48]. Signals with an excitation frequency of 75 kHz indicated the presence of L(0,1) and F(1,1) modes. Wave propagation was examined along the rebar with and without simulated corrosion introduced by partial removal of the concrete surrounding the rebar [49]. The time reversal of wave signal was experimentally used to detect damage in rebar without relying on previous benchmark signals, which are typically impacted by external factors. The signals were generated using piezoelectric ceramics at one end of the rebar, received from the other end, time-reversed in the time domain, and then resent to be captured by the original piezoelectric ceramic. It was concluded that the time reversal process can detect damage of different lengths in rebar embedded in RC since the damage size will ultimately modify the actuated signal.

2.2 Problem Statement and Research Objectives

SHM (structural health monitoring) is becoming more universally recognized as a promising method for enhancing the safety, reliability, and durability of structures. Several destructive and non-destructive techniques were employed to monitor corrosion and its impacts like delamination, pitting, and cracks. Some methods were impractical or unfeasible to be implemented in real constructions. Consequently, none of the corrosion monitoring techniques were shown to be the optimum and ultimate technique, which calls for more investigations and research works to reach a practical, feasible, and reliable monitoring system.

In this research, the UGW technique and FBG strain sensors will be used to monitor the progression of corrosion damage in RC since corrosion will eventually cause delamination between steel and concrete, thus affecting wave propagation and generating stresses in the surrounding concrete. Also, monitoring of the corrosion effect and wave propagation to the adjacent bars will be investigated. In addition to the analysis of the wave leakage to the surrounding concrete, the results of the guided waves will be correlated to the results of embedded FBG. To verify the proposed approach, an impressed voltage technique was used to accelerate the corrosion of steel reinforcement in the RC specimen. The response of the specimens will be monitored to detect the wave characteristics and correlate them with corrosion phases.

CHAPTER 3

METHODOLOGY

3.1 Principle of UGW in Reinforced Concrete

In an infinite isotropic solid medium, there are only two modes of wave propagation: symmetric (Si) and anti-symmetric (Ai). However, when geometric constraints are imposed and the member becomes cylindrical, wave modes will become different and labeled with L, T, and F, which correspond to the longitudinal, torsional, and flexural modes, respectively [50]. These modes are frequency-dependent, and to further distinguish them in cylindrical members, they are characterized by L(n,m), T(n,m), and F(n,m), where n and m are two integers related to the geometric aspects related to the variation in displacement around the circumference of the bar and the sequential mode order, respectively [32, 39, 46]. n=0 specifically indicates that the cylinder is axially symmetric which is the case in the majority of engineering applications that make L(0,m), T(0,m), and F(0,m) the wave modes that attract the greatest attention [50]. Wave propagations are described by phase and group velocities shown in Figure 2.

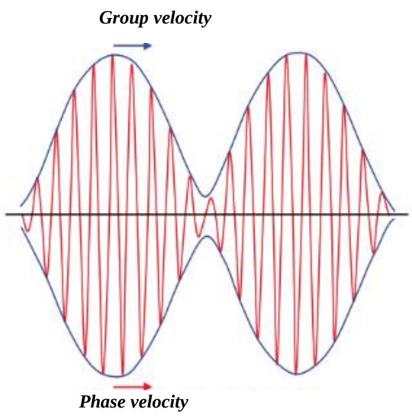

Figure 2 Phase and group velocities

Phase velocity is determined by the movement of a specific "phase" through the waveguide, whereas group velocity refers to the velocity of a wave packet [51]. Dispersion curves, which describe the relationship between the frequency and velocity of a wave, may be used to detect the propagating modes since two or more modes may correspond to a single frequency and as the frequency increases, the number of modes for a certain frequency increase [32]. Figure 3 shows the dispersion curve of a steel bar with a diameter of 10 mm which was simulated using DISPERSE.

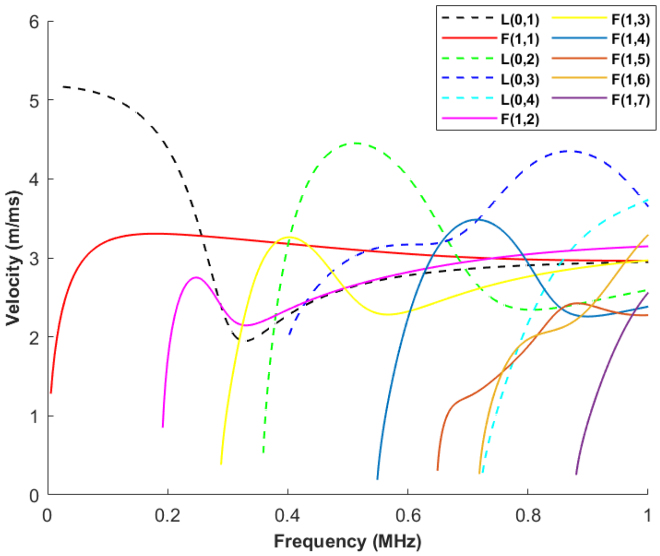

Figure 3 Group velocity dispersion curve of 10 mm bar diameter

Since steel bars are embedded in concrete, which is a heterogenous material, the wave energy may be lost or attenuated due to the leakage of wave energy in the surrounding concrete. Also, reflections of waves at the endpoints of the exposed steel bars and in the contact area between steel and concrete may occur which makes the analysis of the resulting waves more complicated. So, to model the behavior of steel rebar embedded in concrete, it is considered an isotropic solid cylinder embedded in an infinite isotropic medium [52]. However, the main difference is the scattering and leakage of wave energy into the surrounding concrete, which is not typically observed in other multilayered systems [33]. The study of wave propagation characteristics revealed that the velocity of wave propagation along rebar embedded in concrete will be significantly lower than the theoretical velocity for longitudinal waves in bare rebar [53].

3.2 Overview

The test specimens are prepared using a proper mix design and since corrosion is a slow process in nature, accelerated corrosion was achieved by the impressed voltage technique. Then, ultrasonic waves are actuated and sensed across different steel bars, allowing for the observation and analysis of the wave characteristics during different stages of corrosion. The full process followed in the investigation is illustrated in Figure 4.

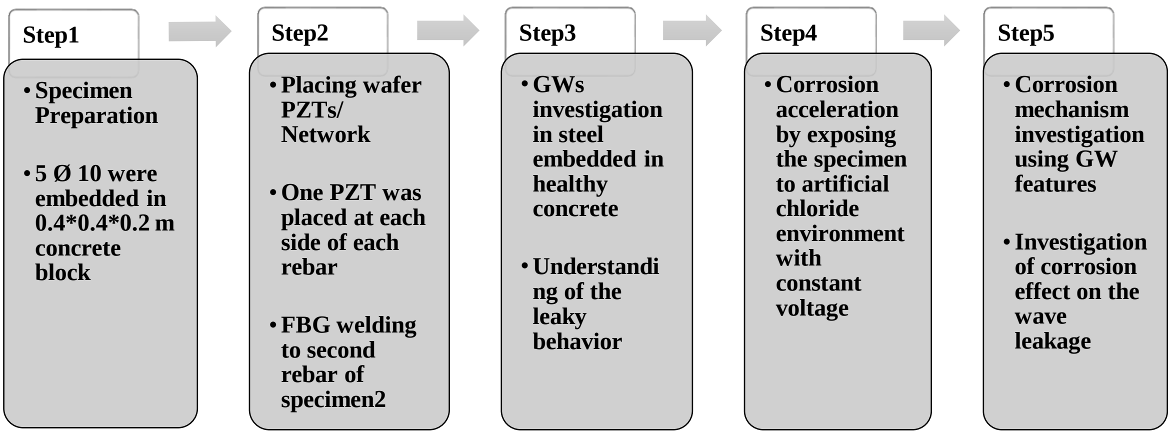

Figure 4 Methodology flowchart

3.2.1 Sample Preparation

In this experiment, two test specimens were prepared using ordinary Portland cement (P.O 42.5), water, coarse aggregates, standard sand, and reinforcing steel. The water-to-cement ratio was 0.5 and the mix proportion of concrete is presented in Table 1. Each of the specimens prepared was 400 mm long, 400 mm wide, and 200 mm high and reinforced with five deformed rebars of 10 mm diameter and 600 mm length of which 400 mm centered embedded length in concrete and 100 mm was outstretched outside the concrete from each side. Additionally, one of the specimens had an embeddable optical strain sensor (OS3600) welded to the second rebar as shown in Figure 5, which would be fully embedded after pouring the concrete. The purpose of placing the fiber Bragg grating (FBG) was to measure the accumulated strain during the corrosion process. The properties of the steel bars used are detailed in Table 1. Before preparing the specimen, the reinforcing bars were cleaned, then fresh concrete was poured into the molds and cured for two days before demolding the specimen, then subsequently put in a normal curing chamber for 14 days. Concrete cylinders have been tested after 7 and 28 days respectively and the average final compressive strength is 21 and 24.8 MPa, respectively. Specimen preparation and detailed dimensions are presented in Figure 6 and Figure 7, respectively.

Table 1 Concrete and steel properties used

Concrete Mix Proportions (kg/m3)	Water	Cement	Fine Aggregates	Coarse Aggregates	
	200	400	700	1150	
Steel bar properties	Diameter	Length	Density	Young’s modulus	Poisson ratio
	10 mm	600 mm	7850 kg/m^3	210 GPa	0.28

Figure 5 Sample with embedded FBG strain sensor

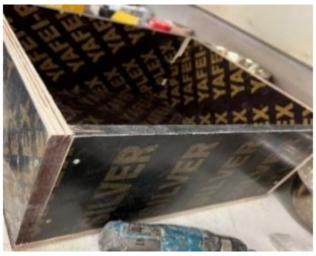

(a) Mold preparation

(b) Steel placement

(c) Concrete pouring

(d) Leveling and tamping

Figure 6 Sample preparation – mold design, reinforcement, and casting

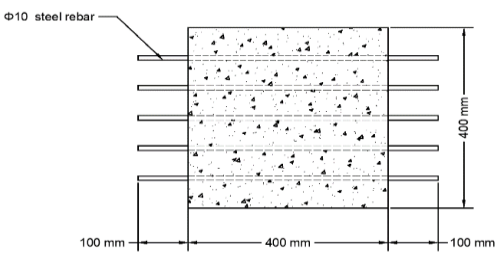

(a) Top view

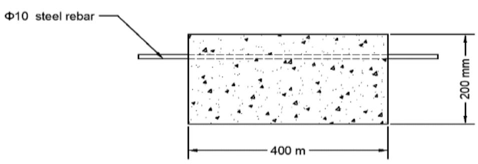

(b) Side view

Figure 7 Reinforced concrete specimen detailing; (a) Top view, (b) Side view

3.2.2 Experiment Set-up

To facilitate the attachments of PZTs, both ends of the steel rebars were smoothed. The rectangular PZTs were then glued 550 mm apart on both ends of the rebar where one end PZT serves as an actuator and the other end PZT serves as a sensor. A typical ultrasonic testing setup for ultrasonic guided wave monitoring is used consisting of a Keysight 33500B signal generator, where the wave packet is produced, PiezoSys® EPA-104 voltage amplifier, and Keysight InfiniiVision DSO-X-3024A oscilloscope, which enables the data collection from the PZTs. The experimental setup with the generation and acquisition systems is shown in Figure 8 with the actuators and sensors connected to the amplifier and oscilloscope devices, respectively.

In this way, it is possible to investigate the change in the transmitted signal compared to a healthy signal due to the degradation of the steel bars resulting from the corrosion. Moreover, to ensure proper representation of the steel rebar embedded in concrete, the steel rebar may be considered as a smooth cylinder when the diameter-to-length ratio is less than 0.4, which is the case in this experiment where the diameter-to-length ratio is 0.018 where the effect of ribs is neglected [47].

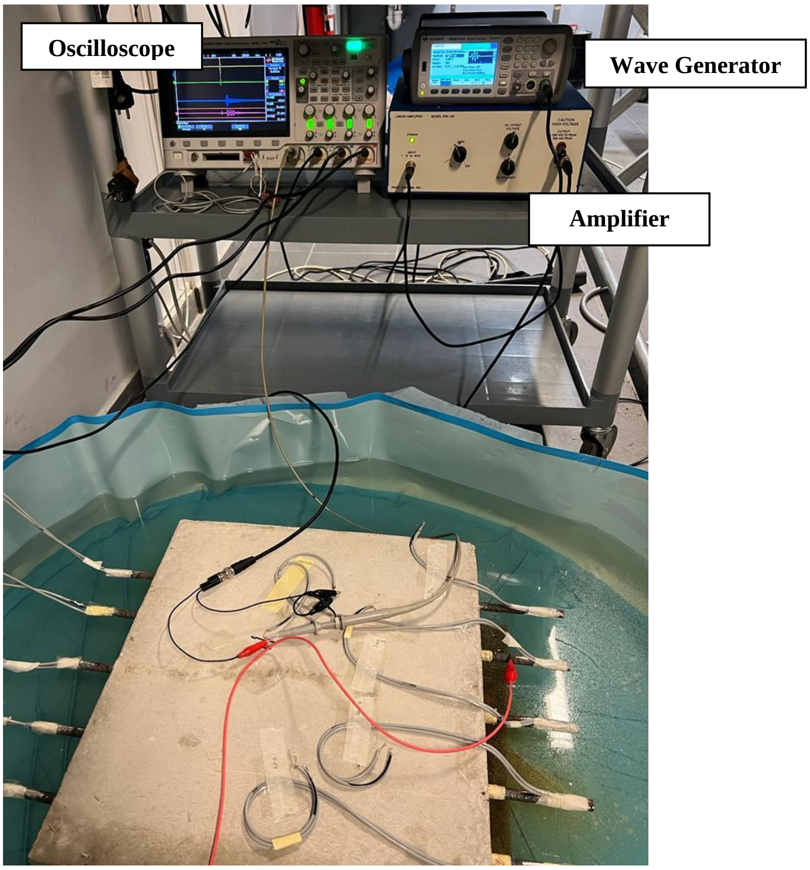

Figure 8 Experimental Setup

In this study, an embeddable optical strain sensor (OS3600) was also used. The sensor is specifically designed for strain measurements along their length, covering a gage length of 30 cm. The sensor also features temperature compensation capabilities to ensure accurate measurements in varying temperature conditions. To withstand harsh environments, the sensor comes with connectors and body protection fittings. The OS3600 sensors are exclusively intended for embedding within concrete structures and they are water resistant which ensures the durability and reliability of these sensors. Experiments were conducted by recording the strain data of the FBG sensor using Optical Sensing Interrogator (Hyperion si255).

3.2.3 Corrosion Initiation

Corrosion is gradual by nature and typically takes a long time. To induce corrosion in the reinforced concrete within a practical timeframe, corrosion is accelerated by exposing the concrete specimen to a chloride environment to obtain a higher amount of corrosion in a shorter period. The specimen is partially immersed in a 3.5% NaCl solution, which acts as an electrolyte. After curing and prior to testing for accelerated corrosion, the specimen was immersed in the NaCl solution for 24 hours to ensure the saturation of the concrete. Then, the second rebar is subjected to corrosion when it was connected to a DC power supply, and a constant voltage of 15V was applied to the steel bar acting as an anode (+), while a stainless-steel plate was positioned in the surrounding solution acting as a cathode (−). The voltage was maintained constant throughout the experiment and the impressed current was measured during the whole experiment [39].

3.2.4 Finite Element Analysis Model

Wave propagation in an intact concrete specimen is evaluated using COMSOL Multiphysics. The Piezoelectric Devices module consists of two separate physics components: Solid Mechanics and Electrostatic which are modeled separately and then combined at the piezoelectric device. The Electrostatics physics module is responsible for solving and detecting the GW generated and received by the PZTs. The wave propagation along the specimen displaces the particles and it is solved using Solid Mechanics physics. The numerical model is simulated on an Intel® Xeon® 2.10 GHz virtual machine with 64 GB RAM and 300 GB disc space.

Figure 9 illustrates the mesh used in the sample model. Typically, the mesh size is determined based on the wavelength derived from dispersion curves at the desired frequency of excitation. To ensure accurate mode conversion, a mesh size of 6 to 10 elements per wavelength is typically recommended [54]. Dispersion curves revealed a minimum wavelength of 14 mm at an excited frequency of 75 kHz. This wavelength value served as a reference for setting the maximum element size, aiming to capture all propagating modes at the excitation frequency. By dividing the wavelength by the minimum element number of six, a maximum element size of 2.33 mm was theoretically determined. However, this desired size was not achievable due to limitations in the workstation's capacity. The piezoelectric transducers used to generate GWs were modeled as piezoelectric transducers of type PZT-5A. The actuated signal is a 5-cycle Hanning window sine wave. The PZT actuator has a voltage with the input signal, while the PZT sensor is grounded with zero voltage with an excitation frequency of 75 kHz.

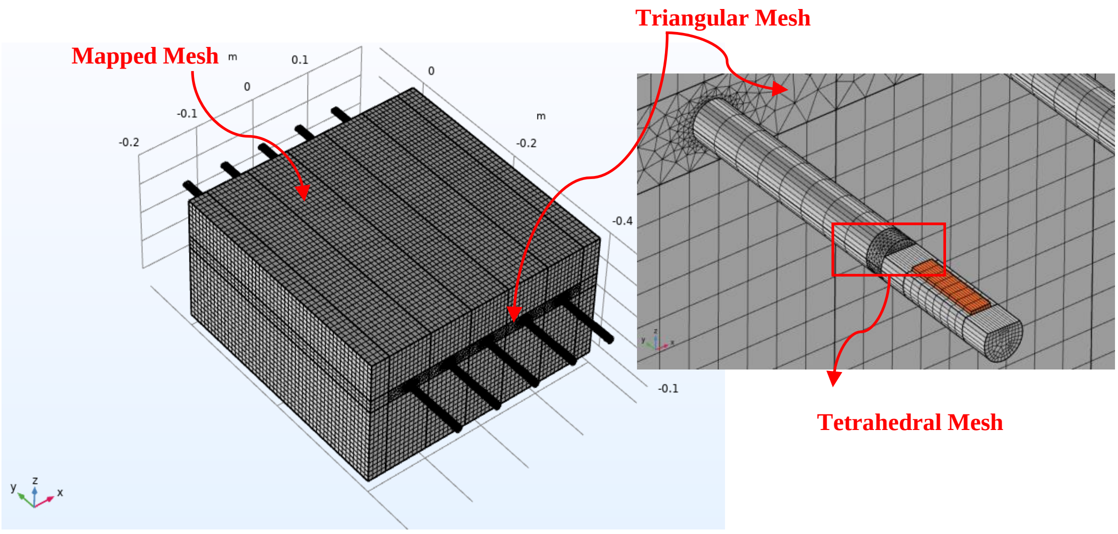

Figure 9 The discretized numerical model in COMSOL Multiphysics

CHAPTER 4

RESULTS AND DISCUSSION

4.1 Introduction

Dispersion curves, which describe the relationship between the frequency and velocity of a wave, may be used to detect the propagating modes since two or more modes may correspond to a single frequency and as the frequency increases, the number of modes for a certain frequency increase. Since steel bars are embedded in concrete, which is a heterogenous material, the wave energy may be lost or attenuated due to the leakage of wave energy in the surrounding concrete. Also, reflections of waves at the endpoints of the exposed steel bars and in the contact area between steel and concrete may occur which makes the analysis of the resulting waves more complicated. The input signal is a 5-cycle sine pulse from the Hanning window. Various excitation frequencies were explored to determine the best frequency of excitation where the responses to various excitation frequencies are studied and displayed in

Figure 10.

The results indicate that an excitation frequency of 75 kHz is the optimal frequency for generating well-defined modes, with the first longitudinal mode being the most prominent. This frequency allows for clear separation and characterization of the different modes in the system under investigation. In addition, previous literature highlighted the sensitivity of the L(0,1) mode to surface defects due to corrosion. The L(0,1) mode proved to be sensitive to surface irregularities and deterioration caused by the corrosion process, making it a reliable indicator for surface defects associated with the corrosion process [33]. Previous literature has explored the use of different frequencies to study bond degradation between steel and concrete. Low-frequency modes, 100 kHz, have shown greater sensitivity in detecting bond degradation. Specifically, the low-frequency fundamental mode L(0,1) is due to its minimal attenuation and higher surface sensitivity [15].

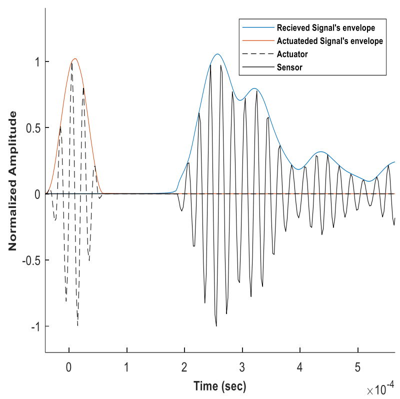

(a) Excitation frequency= 50 kHz

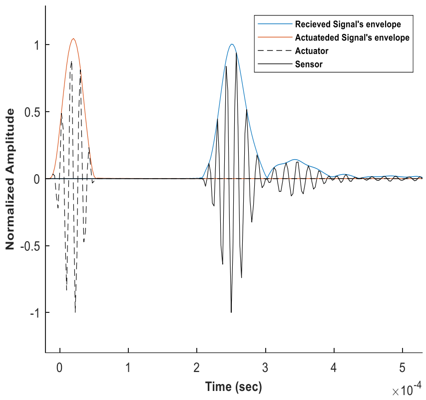

(b) Excitation frequency= 75 kHz

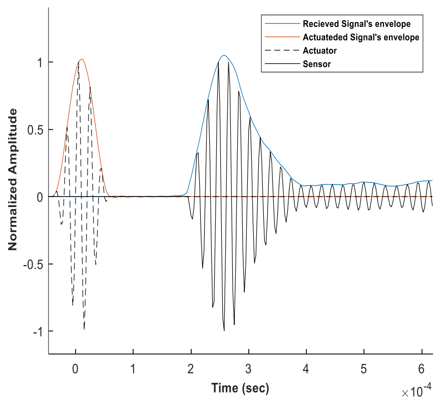

(c) Excitation frequency= 100 kHz

Figure 10 Actuated and received waveforms at different frequencies collected from bar2

4.2 Wave Analysis in Healthy Concrete

4.2.1 Direct Transmission

Figure 11 represents the sensor numberings and distribution over the bars. In this section, the GW through the rebar is investigated on an intact concrete specimen to assess the waveform and the modes propagating, further to search for similarities between the waves guided in parallel bars. Hence, actuation was conducted on five embedded rebars where the PZTs attached at one end of the rebar served as actuators and the PZTs attached to the other end served as sensors. The waves are expected to be guided within the steel bar boundaries, for instance, the actuation by PZT1 will be received by PZT6 along the same rebar from the other side. PZT1 to PZT5 will act as actuators and PZT6 to PZT10 will act as sensors for those actuators, respectively.

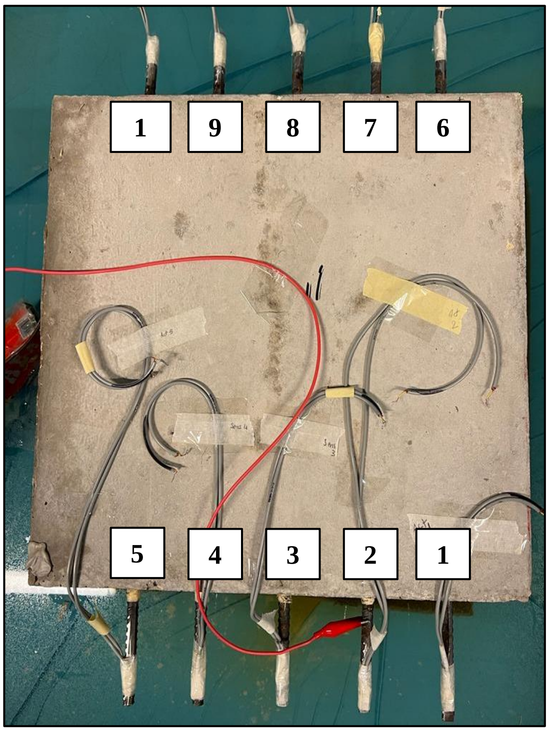

Figure 11 Sensor networks and numbering used

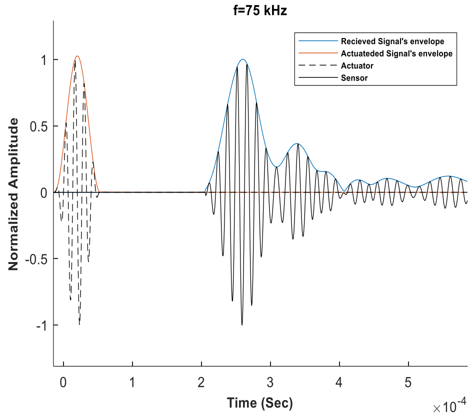

(a) waveform actuated by PZT1 and received by PZT6

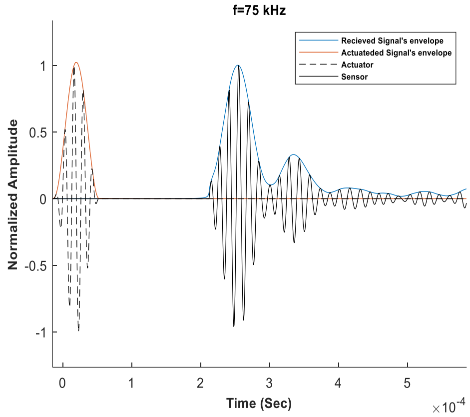

(b) waveform actuated by PZT3 and received by PZT8

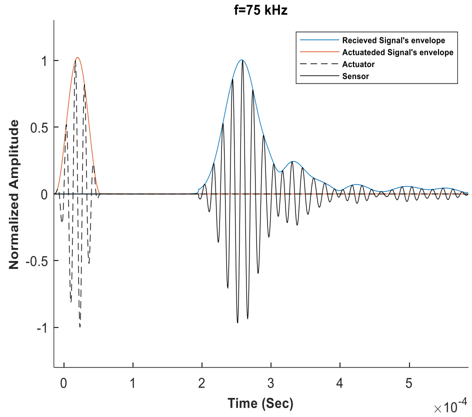

(c) waveform actuated by PZT4 and received by PZT9

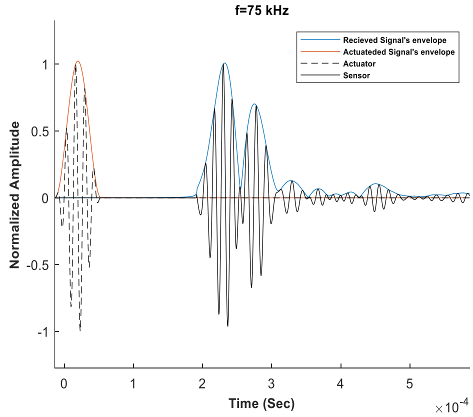

(d) waveform actuated by PZT5 and received by PZT10

Figure 12 Direct Transmission of guided waves in healthy concrete specimen 2 at 75 kHz frequency

Figure 12 displays the signals of UGW propagation in steel surrounded by concrete for Specimen 2 with the first received wave packet being dominant in all bars which propagation was identified as the first longitudinal mode L(0,1), with a calculated velocity of 2291 m/s ± 4%. The direct transmission benchmark results for the first specimen are presented in

Figure 13. Similar benchmark wave packets were captured in both specimens, especially when dealing with the same bar size surrounded by the same concrete properties. However, a noticeable difference presented in Figure 14 was observed in the

received signal of bar 2 in specimen 2, which had a strain FBG sensor welded to it. The presence of the weld has introduced changes that affect the transmitted signals. The velocity of the L(0,1) mode in bar 2 exhibits minimal variation between specimens 1 and 2, with values of 2291.7 m/s and 2303.1 m/s, respectively. However, the amplitude in the second specimen shows a significant reduction of 94.5%.

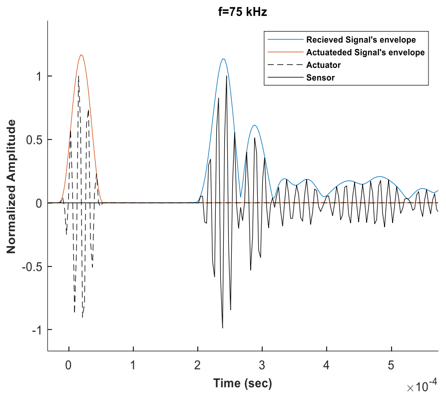

(a) waveform actuated by PZT1 and received by PZT6

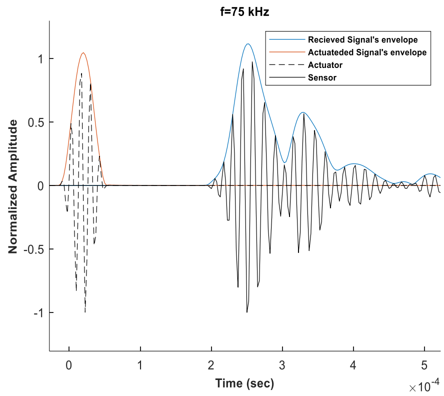

(b) waveform actuated by PZT3 and received by PZT8

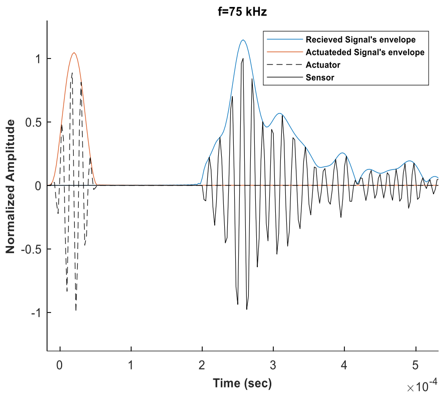

(c) waveform actuated by PZT4 and received by PZT9

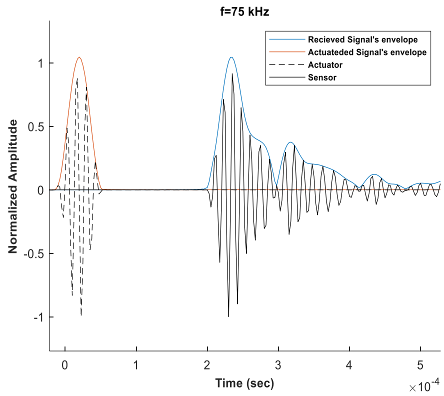

(d) waveform actuated by PZT5 and received by PZT10

Figure 13 Direct Transmission of guided waves in healthy concrete specimen 1 at 75 kHz frequency

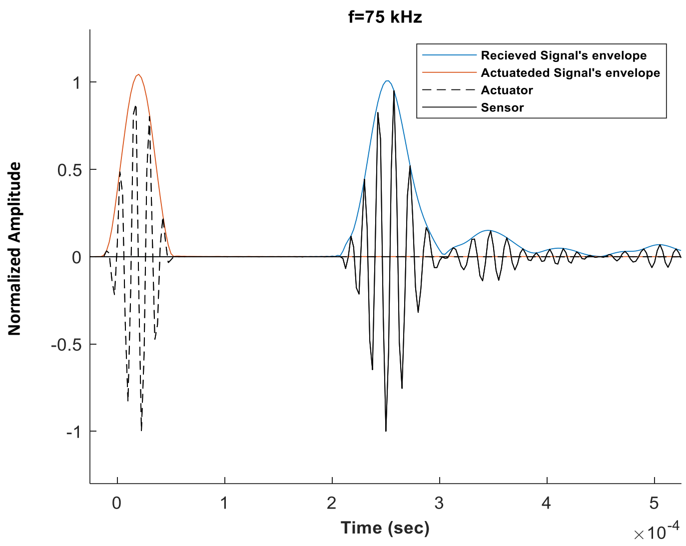

(a) Specimen 1

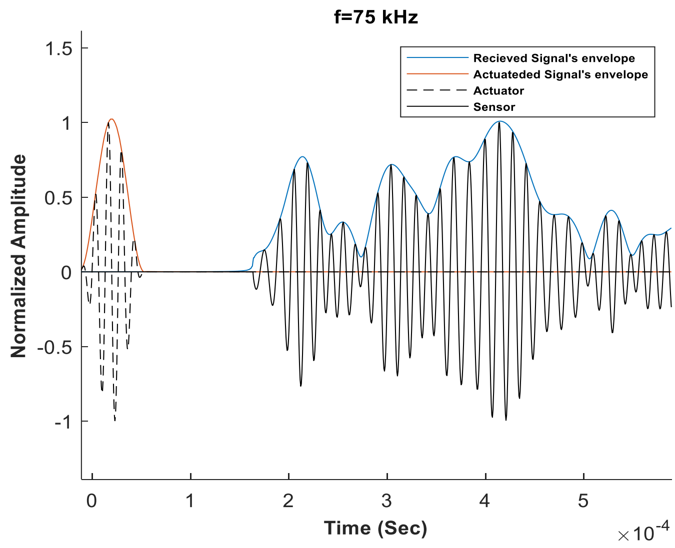

(b) Specimen 2

Figure 14 Waveform actuated by PZT2 and received by PZT7 in both samples.

4.2.2 Leaky Waves

Guided-wave structures may experience wave leakage throughout propagation. Wave leakage is associated with wave guidance, which is highly influenced by a variety of factors such as structural geometry, fill materials, surrounding conditions, and simulation frequency. The leaky behavior of GWs is explored in this part, where the leaked energy in the guided wave system propagates through the surrounding materials (concrete) and is recorded via several receivers. Figure 11 represents the distribution of PZTs that can be utilized as receivers or actuators, where in this part PZT2 serves as an actuator and PZT6, PZT7, PZT8, PZT9, and PZT10 from the facing side serve as sensors.

4.2.2.1 Numerical Work

A multi-physics Finite Element (FE) model was used to demonstrate wave leakage in healthy concrete, and according to Figure 15 it was successfully proved that the wave is leaking to the surrounding concrete once actuating at a single bar.\

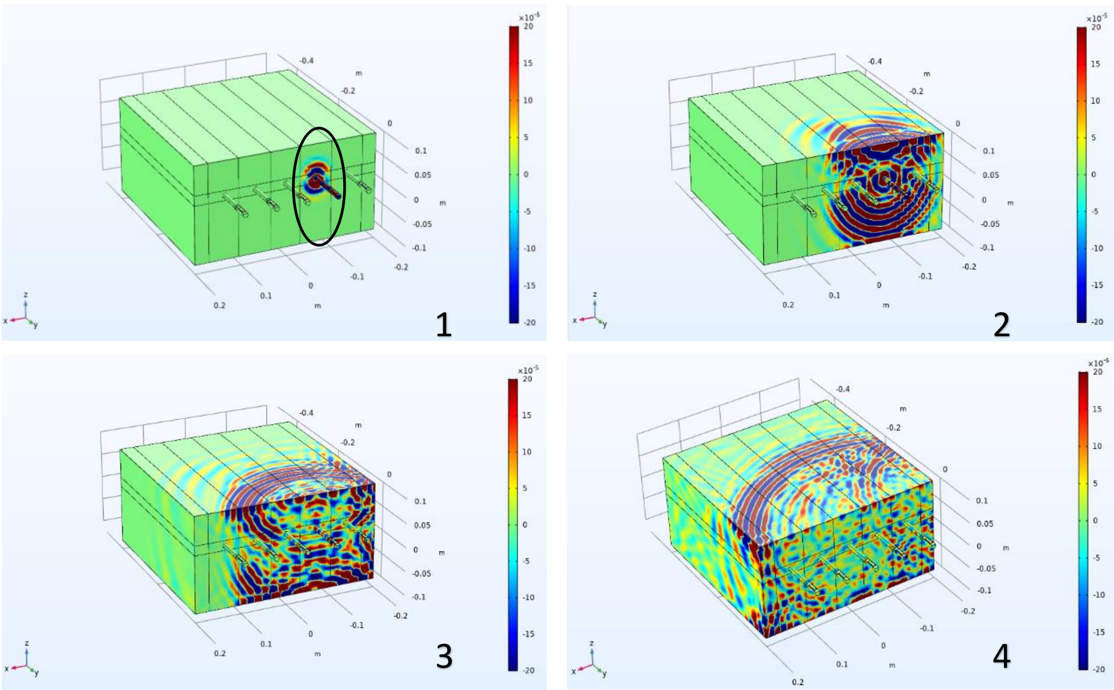

Figure 15 Finite element modeling of wave leakage in healthy concrete.

Once the wave is sent, it propagates through the exposed part of the steel then at the steel-concrete interface, part of the wave is guided through the steel bar, and another part is leaked into the surrounding concrete. The leaked wave then propagates within the concrete medium, and subsequently, waves are transferred to neighboring steel bars, where it is captured. This process of wave propagation, leakage, and transfer between different materials was effectively captured and validated using the FE model, providing insights into the behavior of waves in the concrete structure.

4.2.2.2 Experimental Work

Experimentally, waves were actuated by PZT2 attached to the bar subjected to corrosion and sensed by different PZTs at other bars from the facing side of the bars (see Figure 11). Some of the benchmark signals will be presented and compared to signals received numerically.

Actuating by PZT2 and Receiving by PZT6: Concrete is a heterogeneous material comprising aggregates of different sizes and shapes that are randomly distributed, resulting in complex signals. To analyze these wave packets, peaks were visually identified, with each selected peak potentially representing a specific mode. A comparative analysis of the leakage behavior between experimental observations and numerical simulations in a healthy concrete is presented in Figure 16.

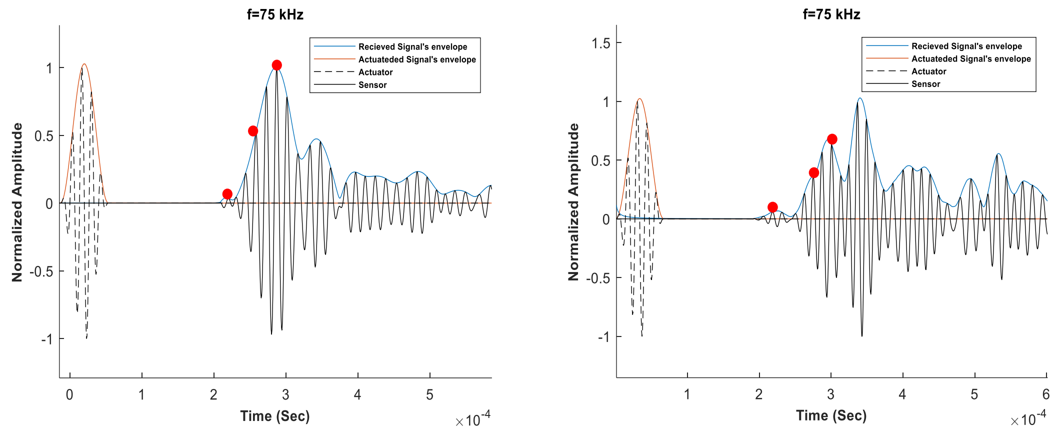

(a) Experimentally (b) Numerically

Figure 16 Waveform actuated by PZT2 and received by PZT6.

The amplitude and velocity of selected modes are presented in Table 2 where the numerical simulations validated the detected modes observed in the experimental results, indicating a clear correlation between the two, noting that the damping effect was not modeled numerically.

Table 2 Velocity (m/s) of Numerically and Experimentally Captured Wave Packets by PZT6.

Peaks	**Velocity (m/s)**	
	Experimental	**Numerical**
1	2728.61	2945.85
2	2295.28	2267.15
3	2050.99	2051.8

Actuating by PZT2 and Receiving by PZT8: By considering different scenarios where Figure 17 displays the captured waves by PZT8. Theoretically, the waveforms captured by PZT8 were expected to resemble those received by PZT6, as both sensors are identical and located at the same distance from the line of actuation. PZT6 is positioned on the right side, while PZT8 is positioned on the left. However, due to the heterogeneous nature of the surrounding concrete, with the presence of aggregates, the received waveforms deviate from this theoretical expectation. The variations in the forms of the received waves can be attributed to the influence of the aggregates. However, we are also able to capture the same modes experimentally and numerically.

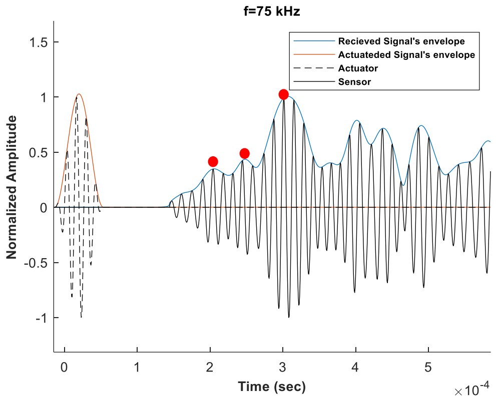

(a) Experimentally

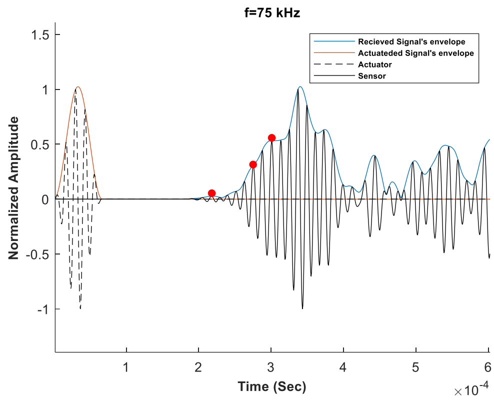

(b) Numerically

Figure 17 Waveform actuated by PZT2 and received by PZT8.

Table 3 Velocity (m/s) of Numerically and Experimentally Captured Wave Packets by PZT8.

Peaks	**Velocity (m/s)**	
	Experimental	**Numerical**
1	2978.05	2941.176
2	2609.89	2553.763
3	2021.84	2050.15

4.3 Effect of corrosion on UGW

4.3.1 Direct Transmission

The embedded rebar in RC beam specimens undergoing corrosion is examined on a regular basis. Ultrasonic pulse transmission signals were recorded daily. Despite the complexity of the received signals, the first peak representing the first longitudinal mode exhibited significant prominence, and fluctuations in amplitude were clearly detectable throughout different corrosion stages. Hence, the corrosion phases depicted in **Error! Reference source not found.** can be correlated with the variations in the amplitude of the L(0,1) mode. An increase or decrease in amplitudes corresponds to one of these phases, namely corrosion initiation following the entry of chloride solution, corrosion propagation and accumulation of rust, and eventual diameter reduction as corrosion progresses. The change in L(0,1) amplitude for the waves guided in bar 2 during the corrosion days of the two specimens is presented in Figure 18.

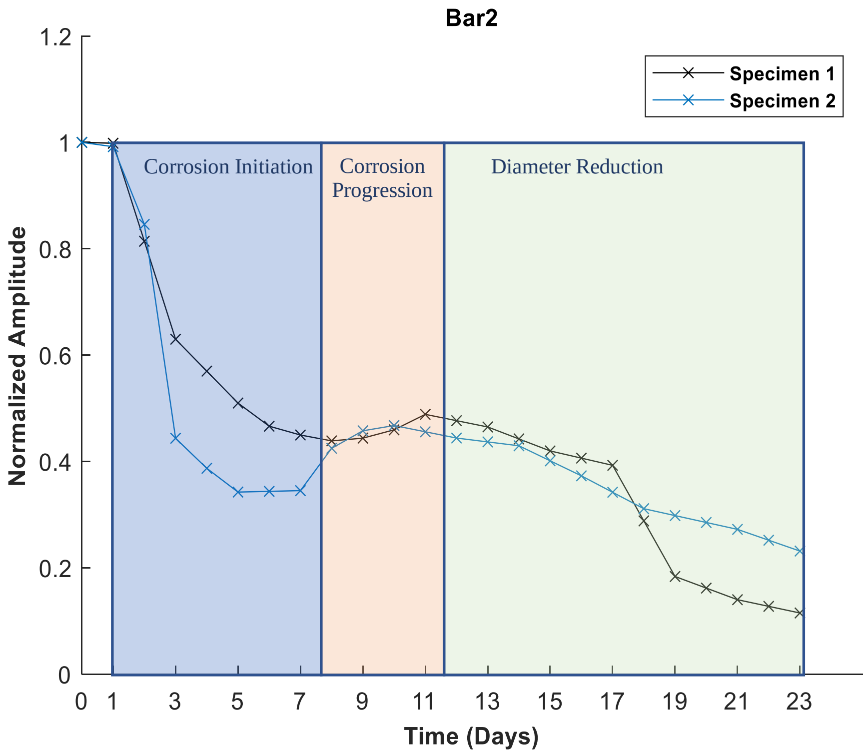

Figure 18 Amplitude variation in L(0,1) mode passing through bar2 with the progress of corrosion

In the early phase of the experiment, the NaCl electrolyte penetrates the concrete specimen through its pores, causing the protective layer around the steel bar to depassivate. On day 2, a change in amplitude was observed in rebar 2 for both specimens. This change in amplitude signifies the initiation of corrosion, as indicated by a decrease in amplitude of 17.87% and 15.42% for specimens 1 and 2, respectively. The reduced amplitude indicates that the bonding between the concrete and steel is becoming stronger, resulting in a higher release of energy into the surrounding concrete medium. The amplitude gradually decreased in the following days until it started to increase on day 9 for specimen 1 and day 8 for specimen 2. The increase in signal amplitude is attributed to the debonding of the rebar from the surrounding concrete, which occurs because of rust formation and the development of internal cracks. This debonding weakens the bonding between the concrete and the rebar, leading to an increase in the signal strength. The specimen was kept in the corrosion setup for additional days, during which a decrease in the amplitude of the L(0,1) mode was observed in both specimens. This reduction in amplitude is attributed to the diameter reduction of the rebar as corrosion progresses. The amplitude continued to decrease by more than 70% of the initial amplitude until day 23 when the experiment was ended for the ultrasound measurements.

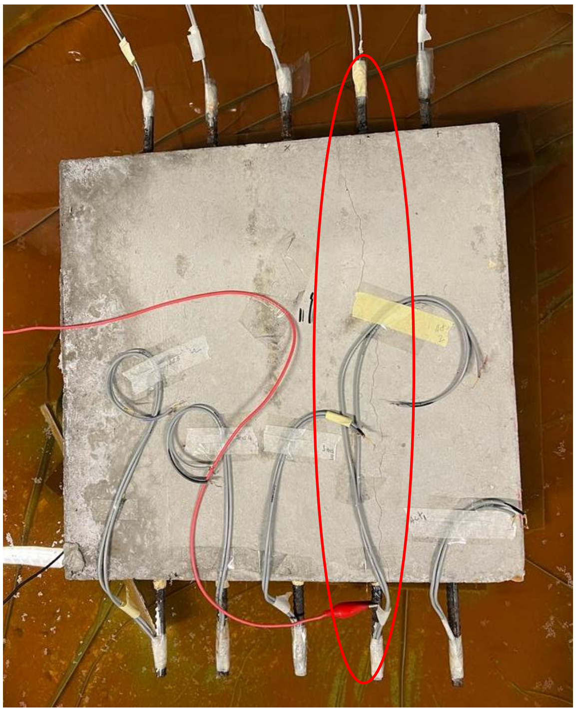

Figure 19 Crack formation in specimen 1

On day 19, a longitudinal crack shown in Figure 19 was observed in specimen 1 along the length of rebar2, where corrosion was induced. The formation of this crack coincided with a sharp drop in the amplitude of the signals received at bar2. As for the second specimen, on day 21, a horizontal crack at the bottom was formed. The crack shown in Figure 20 occurred at a distance from the reinforcement which may be due to the presence of the Fiber Bragg Grating (FBG), which created a rough surface holding the concrete in place. As a result, the stresses were relieved in a different area, far from the reinforcement where the FBG was welded.

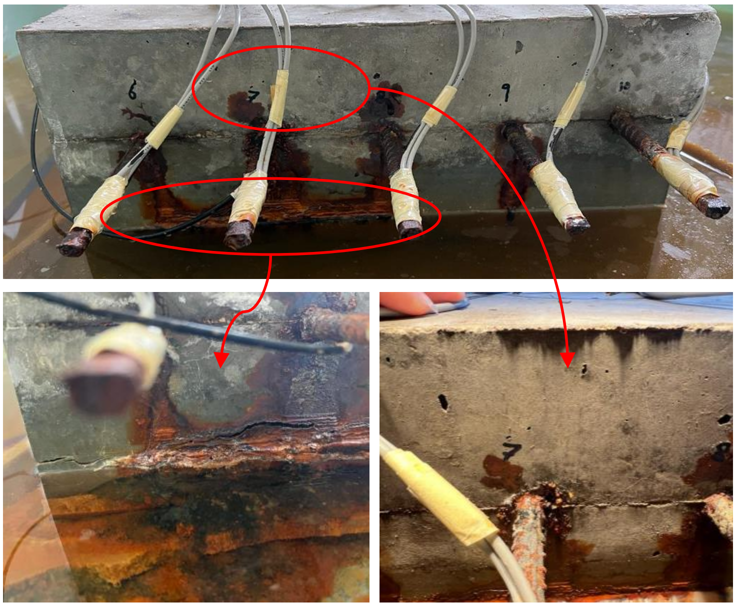

Figure 20 Crack formation along the horizontal direction in specimen 2

Similar patterns were observed for bar 1 and bar 3, as depicted in Figure 21 (a) and (b). The decrease in amplitude began between day 4 and day 5, indicating that corrosion had initiated in the adjacent bars from both sides. Furthermore, according to Figure 22, a rusty color was observed surrounding the bars, confirming the propagation of corrosion to the neighboring bars. Similar trends were identified in bar 4 of specimen 2, where the corrosion phases were analyzed based on the amplitude variation. In contrast, bar 4 in specimen 1 and bar 5 in both specimens 1 and 2, which are located at a greater distance, did not exhibit visible symptoms of corrosion. The decrease in amplitude observed in these bars could be attributed to the expansion of nearby rebars 1, 2, and 3.

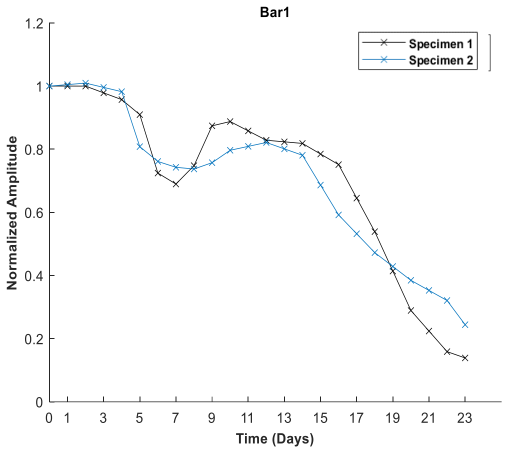

(b) bar1

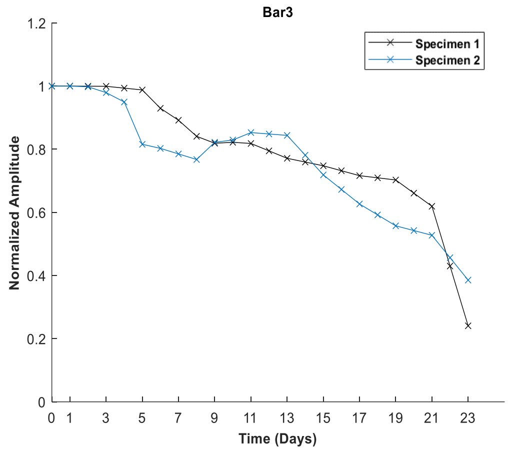

(b) bar3

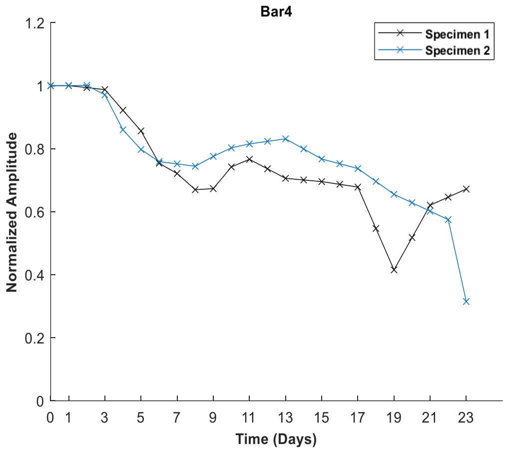

(c) bar4

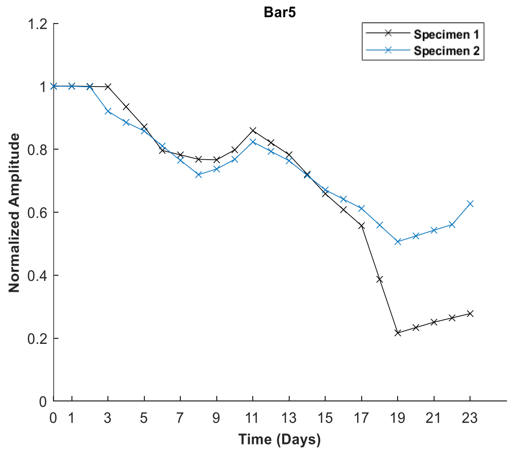

(d) bar5

Figure 21 Amplitude variation in L(0,1) mode passing through neighboring bars with the progress of corrosion.

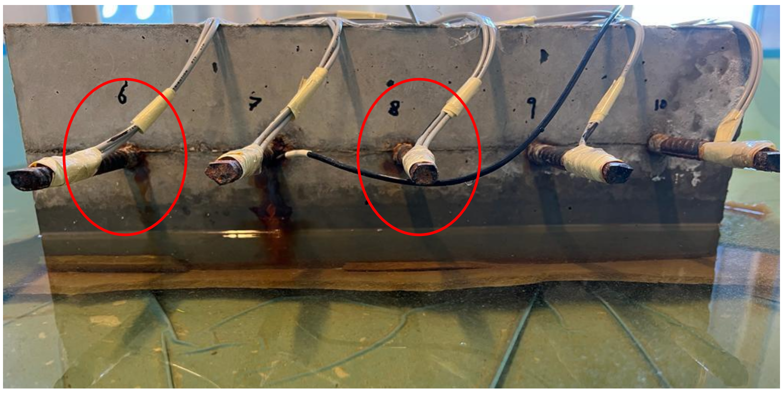

Figure 22 Rusty color at bars 1 and 3

This expansion induces stress within the concrete, consequently decreasing the amplitude of the guided wave as it propagates through the rebar. The rise in signals observed in bars 4 and 5 can be attributed to the debonding of the rebar from the surrounding concrete, which occurs during the corrosion propagation phase in bars 1, 2, and 3. This debonding process weakens the bonding between the concrete and the rebar, leading to an increase in the signal strength. The signals received by PZT8, attached to bar 4, and PZT9, attached to bar 5, exhibit a decrease in amplitude at day 12, indicating the corrosion initiation phase. This is followed by an increase in amplitude on day 19, indicating the corrosion propagation phase.

4.3.2 Leaky Waves

The Ultrasonic Guided Wave Leakage (UGWL) method is employed to monitor the initiation and development of flaws in both steel and concrete. Since the waves propagate through both steel and concrete mediums, it provides valuable information about the condition of the specimen. However, as mentioned before, L(0,1) mode, which was guided through the steel bar, exhibits the highest amplitude and greater sensitivity to corrosion defects. Therefore, the leaky behavior of the L(0,1) mode will be monitored during corrosion. This allows the identification of corrosion defects away from the corrosion source. According to Figure 23 (a) and (b), the amplitude of the L(0,1) mode exhibited a decreasing trend from day 1 to day 9, which can be attributed to the formation of rust at certain locations on the steel bar. As corrosion progresses and the diameter of bar 2 (having the actuator) begins to reduce, more wave energy leaks to the surrounding concrete (as shown in Figure 23 (a) and (b)), and less energy is directed through the rebar (see Figure 18). Subsequently, there was a slight increase in amplitude observed between day 11 and day 14 accompanied by the diameter reduction phase of bar 2, which began on day 12 with a sharp increase detected on day 17. During the diameter reduction phase of bar 2, where the actuator is located, it is observed that the amplitude of the leaked L(0,1) mode increases, as previously presented for PZT6 and PZT8.

When moving away from the source of corrosion, Figure 23 (c) and (d) shows that the signal rise slows down as we move away from the source of corrosion. This is because the signal gets attenuated as it passes through the concrete medium over greater distances. In the first specimen, the signals at PZT9 were no longer detected on day 10, as shown in Figure 23 (c). This loss of signal can be attributed to the formation of major internal along the signal path, resulting in signal loss. The same case was observed in bar 5 of the second specimen on day 11 (refer to Figure 23 (d)).

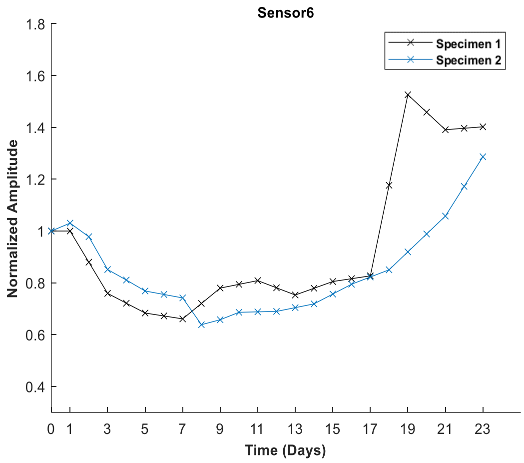

(a) PZT6

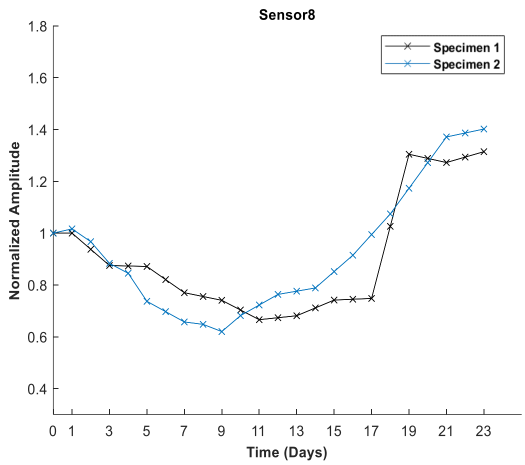

(b) PZT8

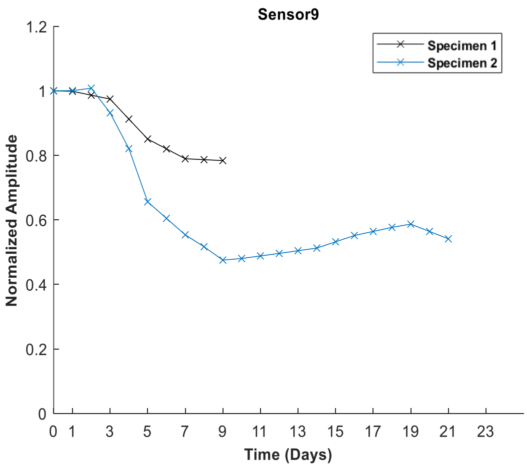

(c) PZT9

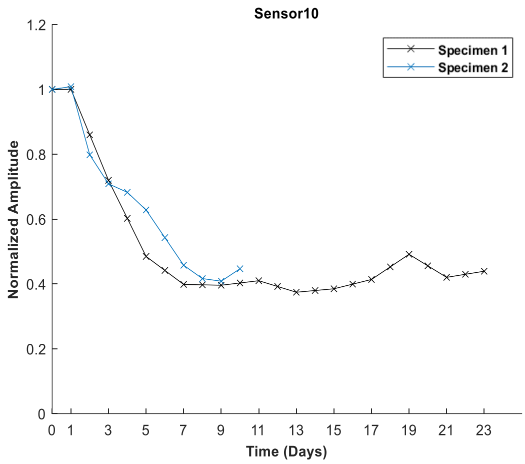

(d) PZT10

Figure 23 Amplitude variation in L(0,1) mode received by different PZTs with the progress of corrosion

When reinforcement corrosion begins due to chloride penetration, typically it takes up to 10 years for the concrete cover surface to deteriorate significantly, requiring repair interventions [55]. However due to the experimentally induced corrosion, bar 2 was highly corroded by day 23 where the wave signals had been completely lost, and the only noise was captured due to the extensive formation of internal cracks. As a result, the analysis of ultrasonic-guided wave signals was discontinued on day 23.

4.4 FBG Strain Measurement

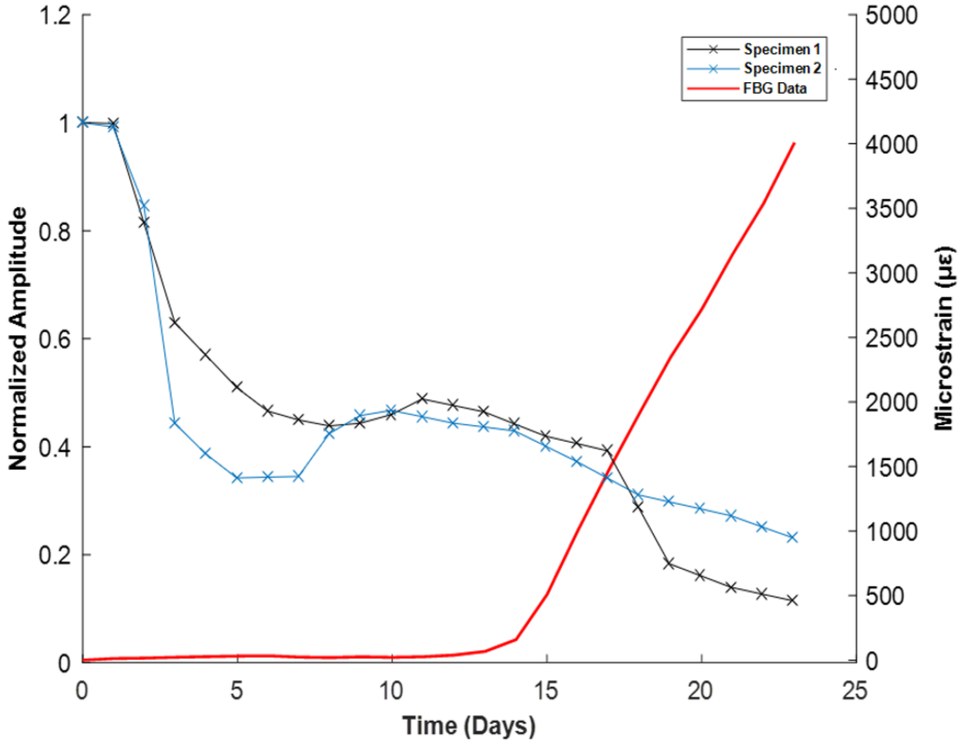

Figure 24 Variation of strain (με) and amplitude in bar 2 with different corrosion days

During the corrosion process, strain measurements were taken using FBG sensors, while simultaneously monitoring the amplitude and velocity variations of the L(0,1) mode propagating in bar 2, which was subjected to corrosion. On day 12, when the diameter reduction phase began, the strain readings started to increase. A reduction in the L(0,1) mode amplitude characterizes this phase, as seen in Figure 24. The diameter reduction phase occurs as corrosion progresses and the steel reinforcement experiences physical changes, such as the development of corrosion products and a decrease in cross-sectional area. These changes result in increased deformations and strain in the surrounding concrete due to the pores being filled with rust products and corrosion continues to progress. Moreover, the velocity change in the L(0,1) mode was initially negligible during the early corrosion stages but became more noticeable in the later stages. This trend is illustrated in Figure 25. In specimen 1, the maximum velocity drop recorded was 7%, indicating a decrease in the propagation velocity of the L(0,1) mode as a result of corrosion. Similarly, in specimen 2, a maximum velocity drop of 9% was observed. These velocity drops suggest that the corrosion process affects the wave propagation characteristics in the steel reinforcement. The increase in the velocity change in the later stages of corrosion may be attributed to several factors, such as the accumulation of corrosion products, changes in the mechanical properties of the corroded steel, or the formation of cracks and defects within the material. These factors can disrupt the uniformity of wave propagation and result in a change in the velocity of the L(0,1) mode.

It is important to note that the recorded increase in strain values reflects the sample's overall expansion rather than being a direct result of tension in the rebar. The observed increase in strain can be attributed to the stresses generated due to the accumulation of corrosion products and the formation of cracks in the surrounding concrete leading to increased strain values.

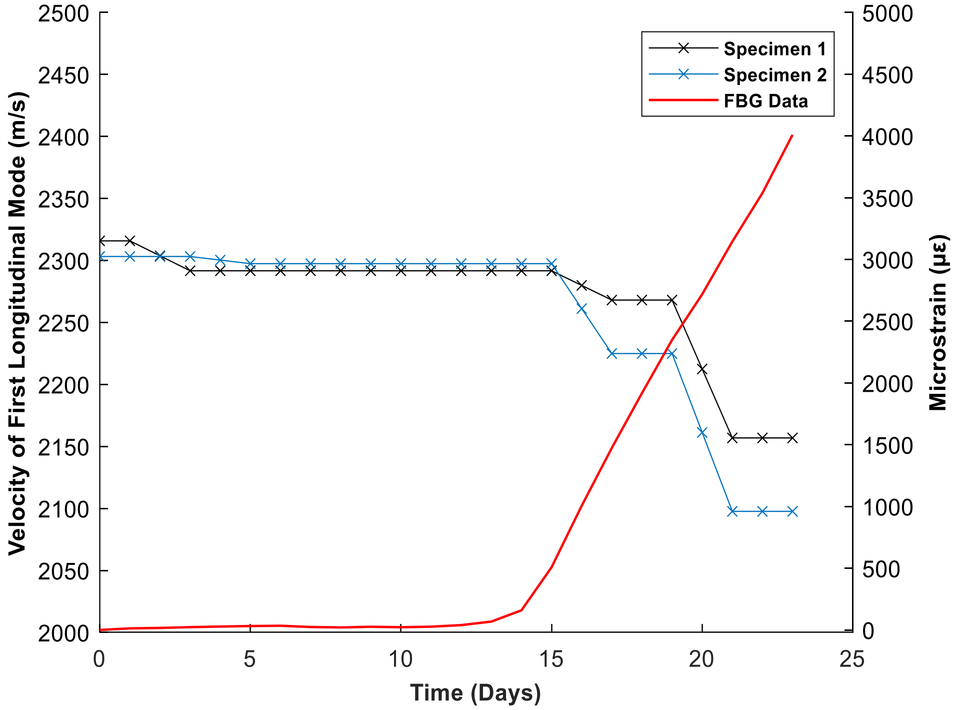

Figure 25 Variation of strain (με) and velocity (m/s) in bar 2 with different corrosion days

CHAPTER 5

CONCLUDING REMARKS

The current study scrutinized the feasibility and reliability of Ultrasonic Guided Waves (UGW) as a non-destructive and early detection method for corrosion in steel reinforcement within concrete structures. By analyzing the pattern of signal strength measurements, the mechanism of corrosion inside the concrete can be deduced. The first longitudinal mode of guided waves showed remarkable sensitivity in detecting different phases of corrosion, including initiation, progression, and diameter reduction phases. The research also revealed that corrosion propagates non-uniformly from the source to neighboring rebars, passing through the concrete medium. Moreover, corrosion can be detected away from the source of corrosion, as wave leakage at the interface occurs with a drop in the sensitivity to the corrosion as we move away from the source. Additionally, the integration of embedded Fiber Bragg Grating (FBG) sensors provided further insights into the correlation between strain and GW readings, particularly during the diameter reduction phase. Furthermore, a multi-physics Finite Element (FE) model successfully demonstrated wave leakage in healthy concrete, which was then validated through experimental verification. These findings contribute to the understanding of corrosion behavior in reinforced concrete structures and provide valuable insights for the development of robust and effective monitoring and maintenance approaches.

The limitation of the current method is its reliance on benchmark signals obtained from healthy concrete where the sensor network needs to be installed before the occurrence of any corrosion. Consequently, further research will be conducted to explore alternative approaches for utilizing Ultrasonic Guided Waves (UGW) in the assessment and monitoring of corrosion in already existing structures. The aim is to develop methodologies that can be applied retrospectively to structures that are already in service, allowing for the evaluation of their corrosion status and facilitating ongoing monitoring.

Future work will involve the integration of a hybrid system for active monitoring that combines UGW techniques with Fiber Bragg Grating (FBG) strain sensors. Furthermore, explore the application of non-linear ultrasound techniques for corrosion detection.

REFERENCES

1. Adrian Forty, F., *Concrete and culture: a material history*. Vol. 43640. 2012: Reaktion Books.
2. McCormac, J.C. and R.H. Brown, *Design of reinforced concrete*. 2015: John Wiley & Sons.
3. Almubaied, O., et al., *Monitoring corrosion process of reinforced concrete structure using FBG strain sensor.* IEEE Transactions on Instrumentation and Measurement, 2017. **66**(8): p. 2148-2155.
4. Alhamad, O. and W. Eid, *Reinforced concrete problems and solutions: A literature review.* Journal of Construction Materials, 2020. **2**: p. 1-1.
5. Moussard, M., P. Garibaldi, and M. Curbach. *The invention of Reinforced concrete (1848–1906)*. in *High Tech Concrete: Where Technology and Engineering Meet: Proceedings of the 2017 fib Symposium, held in Maastricht, The Netherlands, June 12-14, 2017*. 2018. Springer.
6. Nawy, E.G., *Concrete construction engineering handbook*. 2008: CRC press.
7. Gardner, D., et al., *A survey on problems encountered in current concrete construction and the potential benefits of self-healing cementitious materials.* Case studies in construction materials, 2018. **8**: p. 238-247.
8. Hobson, G. and D. Grierson, *Tomato*. 1993: Springer.
9. Oloke, O.C., et al., *Incessant building collapse in Nigeria: a framework for post-development management control.* Developing Country Studies, 2017. **7**(3): p. 114-127.
10. Puri, V. and S. Prakash, *Foundations for Dynamic Loads.* Geotechnical Special Publication, 2010.
11. Epaarachchi, D.C. and M.G. Stewart, *Human Error and Reliability of Multistory Reinforced-Concrete Building Construction.* Journal of Performance of Constructed Facilities, 2004. **18**(1): p. 12-20.
12. Luković, M., et al., *Failure modes in concrete repair systems due to ongoing corrosion.* Advances in Materials Science and Engineering, 2017. **2017**.
13. Poursaee, A., *Corrosion measurement and evaluation techniques of steel in concrete structures*. 2016. p. 169-191.
14. Gjørv, O.E., *Durability of Concrete Structures.* Arabian Journal for Science and Engineering, 2011. **36**(2): p. 151-172.
15. Sharma, A., et al., *Investigation of deterioration in corroding reinforced concrete beams using active and passive techniques.* Construction and Building Materials, 2018. **161**: p. 555-569.
16. Apostolopoulos, C., *The Consequences of Chloride-Induced Corrosion on Steel Bar and Reinforced Concrete Structures.* Journal of Applied Mechanical Engineering, 2012. **01**.
17. Tan, C., et al., *Fiber Bragg grating based sensing system: Early corrosion detection for structural health monitoring.* Sensors and Actuators A: Physical, 2016. **246**: p. 123-128.
18. Montemor, M., A. Simões, and M. Ferreira, *Chloride-induced corrosion on reinforcing steel: From the fundamentals to the monitoring techniques.* Cement and Concrete Composites, 2003. **25**: p. 491-502.
19. Broomfield, J.P. *Corrosion of Steel in Concrete: Understanding, Investigation and Repair, Second Edition*. 2003.

20. Hu, W., et al., *Fe–C-coated fibre Bragg grating sensor for steel corrosion monitoring.* Corrosion Science, 2011. **53**: p. 1933-1938.
21. Gupta, S., *Comparison of Non-Destructive and Destructive Testing on Concrete: A Review.* Trends in Civil Engineering and its Architecture, 2018. **3**.
22. Workman, G. and O. Moore, *Nondestructive Testing Handbook 10. Overview: Columbus, American Society of Nondestructive Testing*. 2012.
23. Luo, D., J. Li, and Y. Li. *A review of fiber-optic corrosion sensor in civil engineering*. in *AIP Conference Proceedings*. 2018. AIP Publishing LLC.
24. Garbacz, A., L. Courard, and B. Bissonnette, *A surface engineering approach applicable to concrete repair engineering.* Bulletin of the Polish Academy of Sciences: Technical Sciences, 2013: p. 73-84-73-84.
25. Helal, J., M. Sofi, and P. Mendis, *Non-destructive testing of concrete: A review of methods.* Electronic Journal of Structural Engineering, 2015. **14**(1): p. 97-105.
26. Sajid, S. and L. Chouinard, *Impulse response test for condition assessment of concrete: A review.* Construction and Building Materials, 2019. **211**: p. 317-328.
27. Hoła, J., J. Bień, and K. Schabowicz, *Non-destructive and semi-destructive diagnostics of concrete structures in assessment of their durability.* Bulletin of the Polish Academy of Sciences. Technical Sciences, 2015. **63**(1): p. 87--96.
28. Colangelo, F., R. Cioffi, and I. Farina, *Handbook of sustainable concrete and industrial waste management: recycled and artificial aggregate, innovative eco-friendly binders, and life cycle assessment*. 2021: Woodhead Publishing.
29. No, T.C.S., *Guidebook on non-destructive testing of concrete structures.* Training Course Series, 2002.
30. Tomita, K. and M.Y.L. Chew, *A Review of infrared thermography for delamination detection on infrastructures and buildings.* Sensors, 2022. **22**(2): p. 423.
31. Truong-Hong, L., R. Lindenbergh, and T.A. Nguyen, *Structural assessment using terrestrial laser scanning point clouds.* International Journal of Building Pathology and Adaptation, 2022. **40**(3): p. 345-379.
32. Li, D., et al., *Corrosion monitoring and evaluation of reinforced concrete structures utilizing the ultrasonic guided wave technique.* International Journal of Distributed Sensor Networks, 2014. **10**(2): p. 827130.
33. Ervin, B.L. and H. Reis, *Longitudinal guided waves for monitoring corrosion in reinforced mortar.* Measurement Science and Technology, 2008. **19**(5): p. 055702.
34. Elsener, B., et al., *Half-cell potential measurements—Potential mapping on reinforced concrete structures.* Materials and Structures, 2003. **36**(7): p. 461-471.
35. Martínez, I. and C. Andrade, *Examples of reinforcement corrosion monitoring by embedded sensors in concrete structures.* Cement and Concrete Composites, 2009. **31**(8): p. 545-554.
36. Duffó, G., et al., *Application of gamma-ray radiography and gravimetric measurements after accelerated corrosion tests of steel embedded in mortar.* Cement and Concrete Research, 2015. **74**: p. 1-9.
37. Li, W., et al., *Monitoring concrete deterioration due to reinforcement corrosion by integrating acoustic emission and FBG strain measurements.* Sensors, 2017. **17**(3): p. 657.

38. Zaki, A., et al., *Non-destructive evaluation for corrosion monitoring in concrete: A review and capability of acoustic emission technique.* Sensors, 2015. **15**(8): p. 19069-19101.
39. Bremer, K., et al., *Fibre Optic Sensors for the Structural Health Monitoring of Building Structures.* 3RD INTERNATIONAL CONFERENCE ON SYSTEM-INTEGRATED INTELLIGENCE: NEW CHALLENGES FOR PRODUCT AND PRODUCTION ENGINEERING, 2016. **26**: p. 524-529.
40. Grattan, S., et al. *Fibre Bragg grating sensors for reinforcement corrosion monitoring in civil engineering structures*. in *Journal of Physics: Conference Series*. 2007. IOP Publishing.
41. Gao, J., et al., *Monitoring of corrosion in reinforced concrete structure using Bragg grating sensing.* Ndt & E International, 2011. **44**(2): p. 202-205.
42. Fan, G.-X., et al., *Strain Conditions Monitoring on Corroded Prestressed Steel Strands in Beams Based on Fiber Bragg Grating Sensors.* Sensors, 2020. **20**(8): p. 2288.
43. Sharma, A., et al., *Ultrasonic guided waves for monitoring corrosion of FRP wrapped concrete structures.* Construction and Building Materials, 2015. **96**: p. 690-702.
44. Bogas, J.A., M.G. Gomes, and A. Gomes, *Compressive strength evaluation of structural lightweight concrete by non-destructive ultrasonic pulse velocity method.* Ultrasonics, 2013. **53**(5): p. 962-972.
45. Ervin, B.L., et al. *Monitoring uniform and localized corrosion in reinforced mortar using high-frequency guided longitudinal wages*. in *Sensors and Smart Structures Technologies for Civil, Mechanical, and Aerospace Systems 2008*. 2008. SPIE.
46. Miller, T.H., et al., *A new guided wave–based technique for corrosion monitoring in reinforced concrete.* Structural Health Monitoring, 2013. **12**(1): p. 35-47.
47. Li, D., T. Ruan, and J. Yuan, *Inspection of reinforced concrete interface delamination using ultrasonic guided wave non-destructive test technique.* Science China Technological Sciences, 2012. **55**: p. 2893-2901.
48. Sriramadasu, R.C., Y. Lu, and S. Banerjee, *Identification of incipient pitting corrosion in reinforced concrete structures using guided waves and piezoelectric wafer transducers.* Structural Health Monitoring, 2019. **18**(1): p. 164-171.
49. Mustapha, S., et al., *Damage detection in rebar-reinforced concrete beams based on time reversal of guided waves.* Structural Health Monitoring, 2014. **13**(4): p. 347-358.
50. Su, Z. and L. Ye, *Identification of damage using Lamb waves: from fundamentals to applications*. Vol. 48. 2009: Springer Science & Business Media.
51. Lei, Y. and Z.-P. Zheng, *Review of physical based monitoring techniques for condition assessment of corrosion in reinforced concrete.* Mathematical Problems in Engineering, 2013. **2013**.
52. Reis, H., et al., *Estimation of corrosion damage in steel reinforced mortar using guided waves.* 2005.
53. Ervin, B.L., et al., *Estimation of general corrosion damage to steel reinforced mortar using frequency sweeps of guided mechanical waves.* Insight-Non-Destructive Testing and Condition Monitoring, 2006. **48**(11): p. 682-692.
54. Marburg, S., *Six boundary elements per wavelength: Is that enough?* Journal of computational acoustics, 2002. **10**(01): p. 25-51.

55. Delatte, N., *Failure, distress and repair of concrete structures*. 2009: Elsevier.